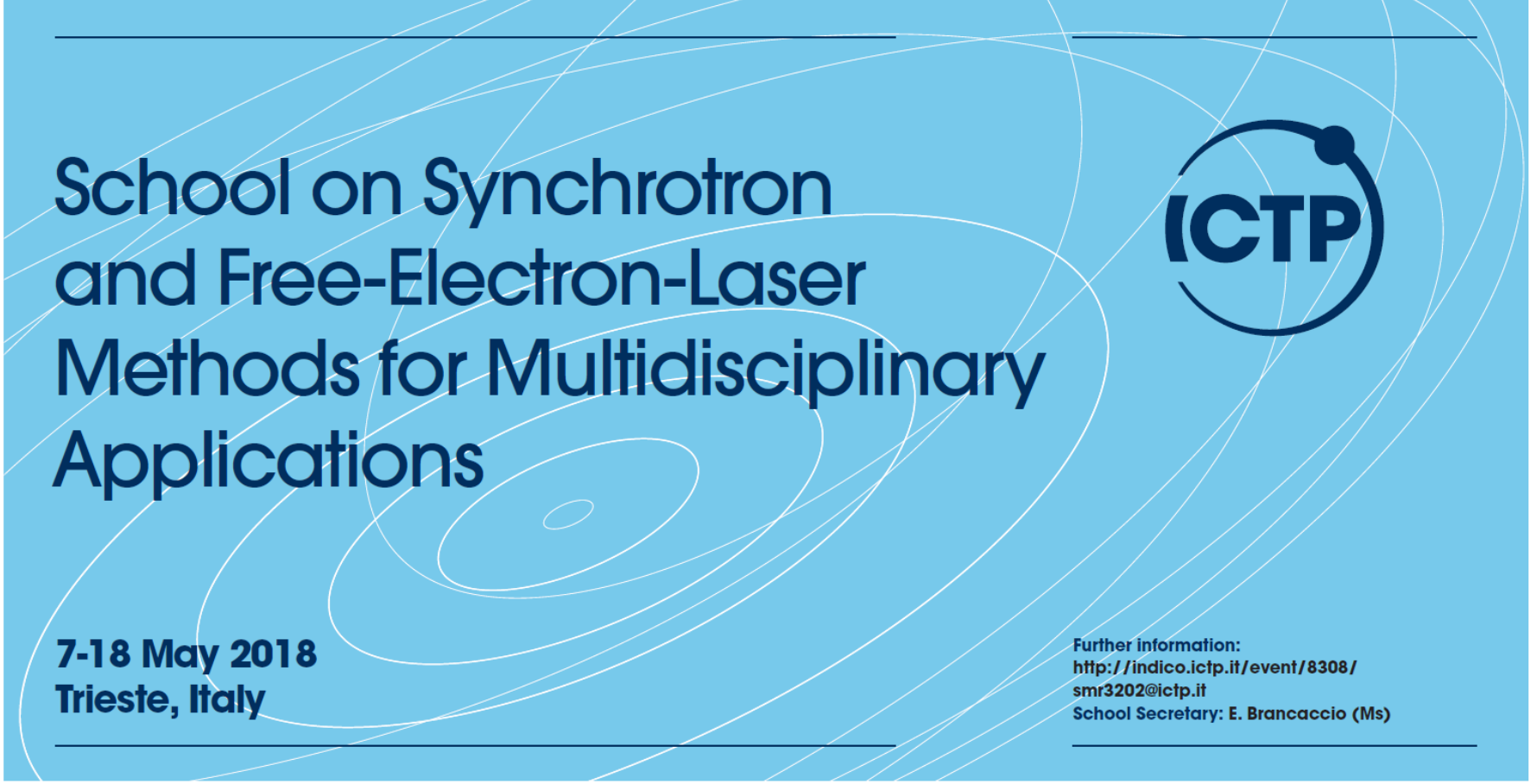

Application of XAS: from Materials Sciences to Cultural Heritage

Giuliana Aquilanti
giuliana.aquilanti@elettra.eu

School on Synchrotron and Free-Electron-Laser Methods for Multidisciplinary Applications

7-18 May 2018
Trieste, Italy

Further information:
http://indico.ictp.it/event/8308/
smr3202@ictp.it
School Secretary: E. Brancaccio (Ms)

X-ray absorption spectroscopy applied to operando and time resolved studies

Giuliana Aquilanti
giuliana.aquilanti@elettra.eu

Elettra Sincrotrone Trieste

Time-resolved studies

- The phenomena of temporal changes have been one the most fundamental concepts of science from the origins to the modern physics
- Temporal changes investigated by scientific methods occur on timescales of more than 30 orders of magnitude

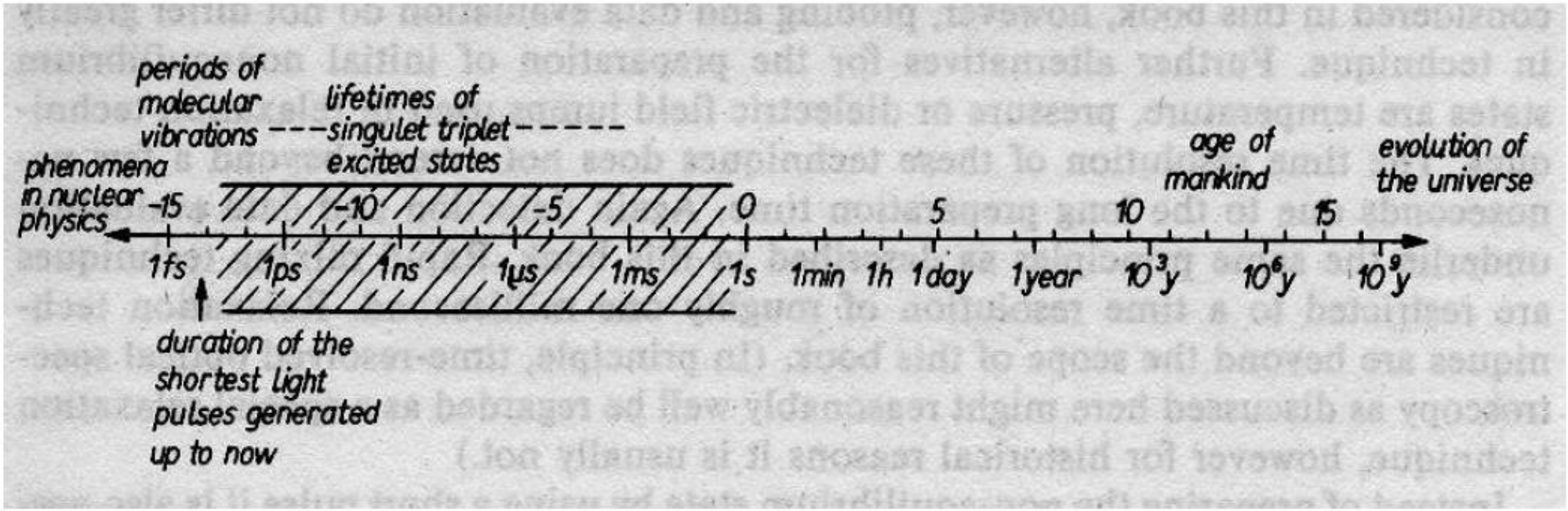

Elettra Sincrotrone Trieste

Outline

- **Energy scanning XAS**
  - Operando LiS battery
  - Magnetite biomineralization in bacteria
- **Quick EXAFS**
  - Nucleation of Au NPs
  - Structural kinetics of Pt/C cathode catalyst
- **Energy dispersive XAS**
  - Photoinduced excited states in complexes
  - Iron melting at high pressure

Elettra Sincrotrone Trieste

Outline

- **Energy scanning XAS**
  - Operando LiS battery
  - Magnetite biomineralization in bacteria
- **Quick EXAFS**
  - Nucleation of Au NPs
  - Structural kinetics of Pt/C cathode catalyst
- **Energy dispersive XAS**
  - Magnetism at extreme magnetic fields
  - Photoinduced excited states in complexes
  - Iron melting at high pressure

Energy scanning XAS spectrometer

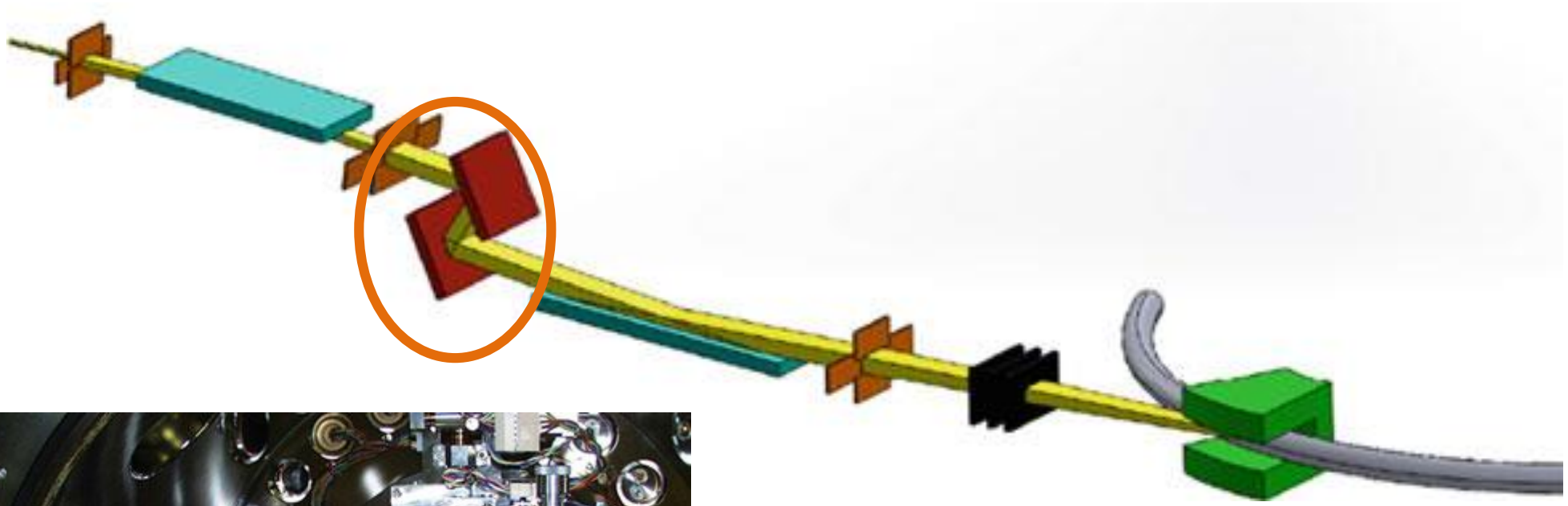

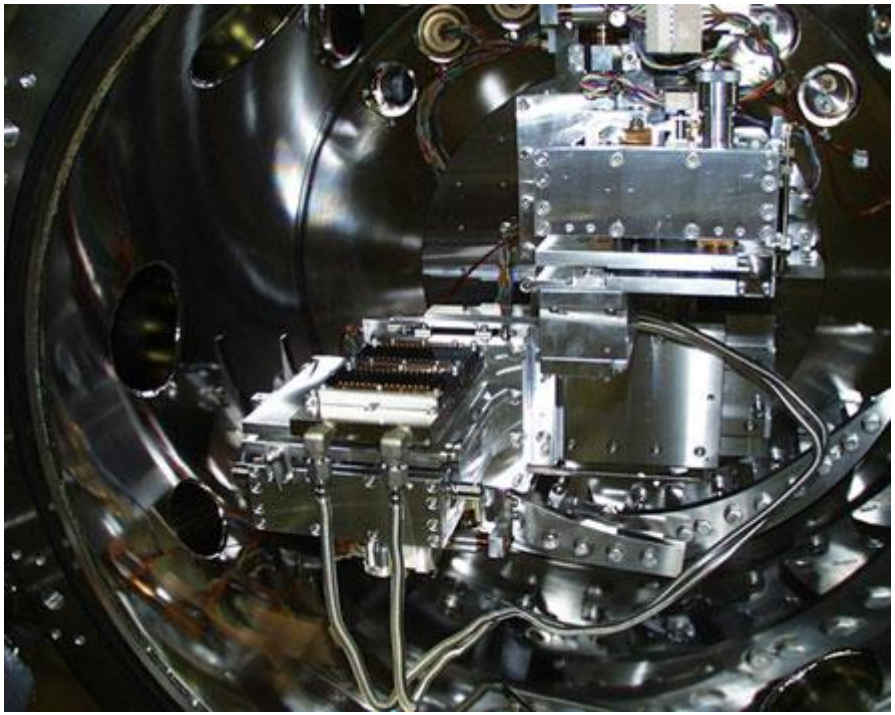

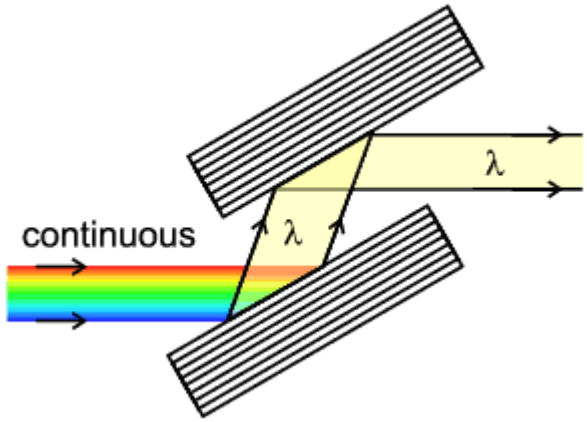

Operando XAS study of LiS batteries

(Simplified) electrochemical reactions between Li and S:

$$S_8 + Li^+ + e^- \rightarrow Li_2S_x \text{ (2.4 – 2.1 V)}$$
$$Li_2S_x + Li^+ + e^- \rightarrow Li_2S_2 \text{ and/or } Li_2S \text{ (2.1 – 1.5 V)}$$

The reactions include solid-liquid-solid transformation, causing great complexity

Advantages and disadvantages

Advantages

- High energy density (2600 W h kg^{-1})
- High capacity (1642 mA h/g)
- Low cost (S is abundant)
- Environmental friendliness

Disadvantages

- Poor conductivity of S
- Volume variation of S (→ capacity fading)
- Polysulfide shuttle mechanism
- **Short lifetime**

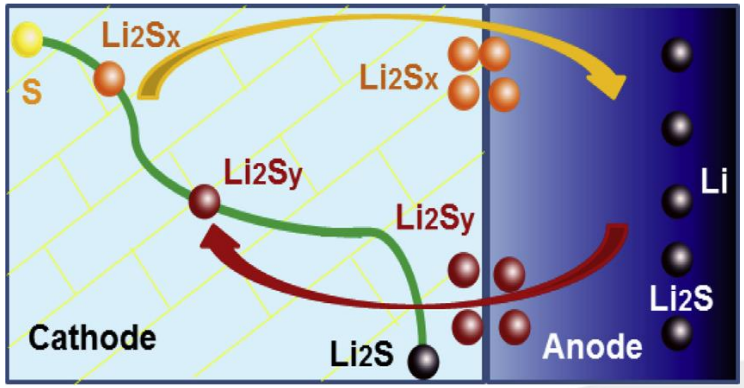

Cheng et al. (2014)
J. Power Sour. **253**, 263

Cell and chamber

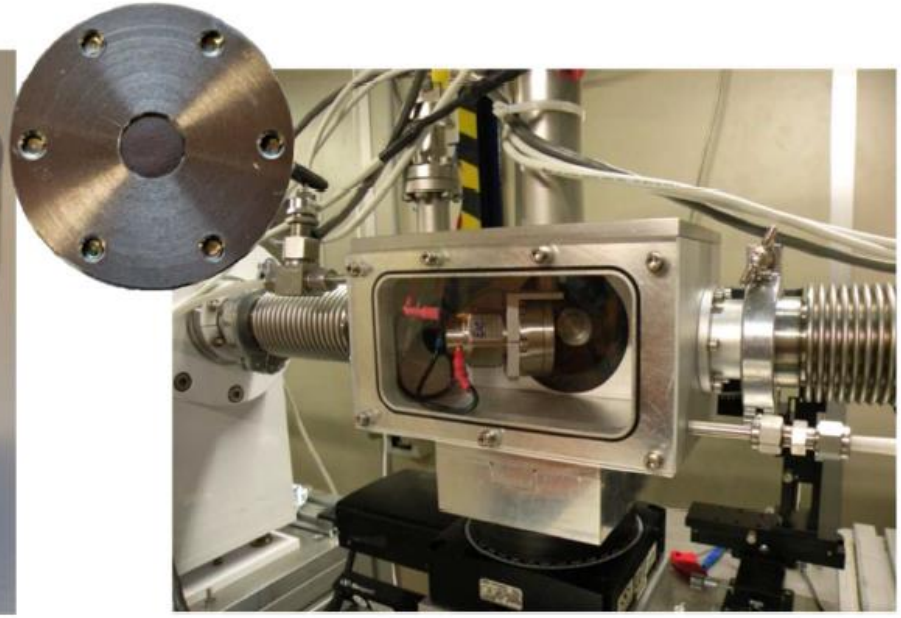

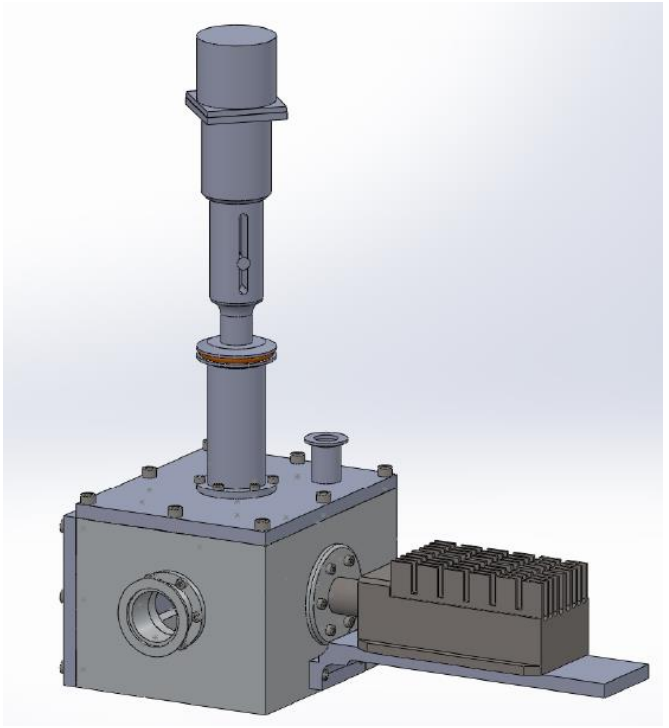

- Modified 4-electrodes Swagelok® cell with 13 μm thick Be window
- Chamber with He overpressure

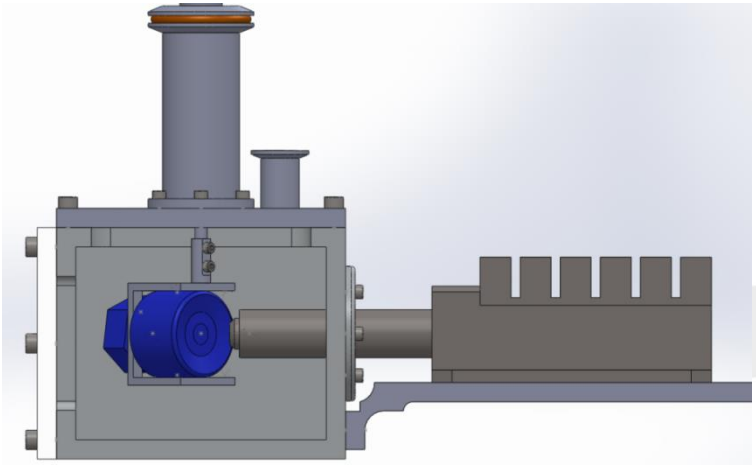

Experimental details

Measurements

- XAFS beamline at Elettra
- S K-edge
- Fluorescence mode

Samples

- Individual components of the battery (cathode, polysulfides, electrolyte)
- Battery in operando conditions

Operando measurements

Cathode composite

- MnS-1 (4.5 wt %)
- Printex XE2 (Degussa) carbon black (70.5 wt %)
- sulfur (25 wt %)

Composite:PTFE: carbon black (8:1:1) in isopropanol solvent was casted in an Al foil using the doctor-blade technique

Electrolyte

- 1M LiTDI in TEGDME:DOL (tetra(ethylene glycol) dimethyl ether:1,3-dioxolane)

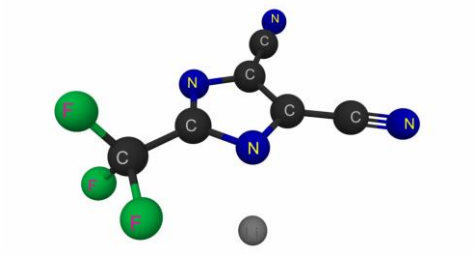

R. Dominko et al.(2015)
J. Phys. Chem. C **119**, *19001-19010*

Operando XANES results

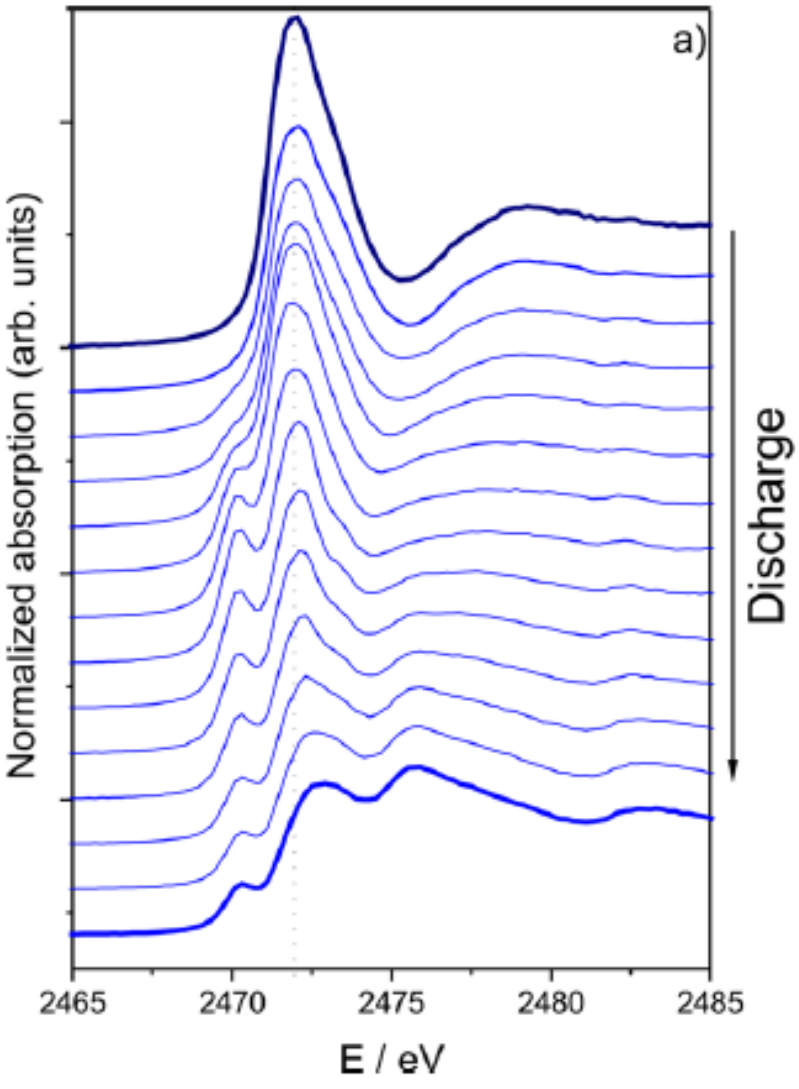

- 1 spectrum/65 min (C/20 rate per electron, i.e. $\Delta x \sim 0.054$ in Li_xS)
- Three components: S, PS Li_2S
- Linear combination fitting using the three components extracted directly from the set of operando spectra of the battery

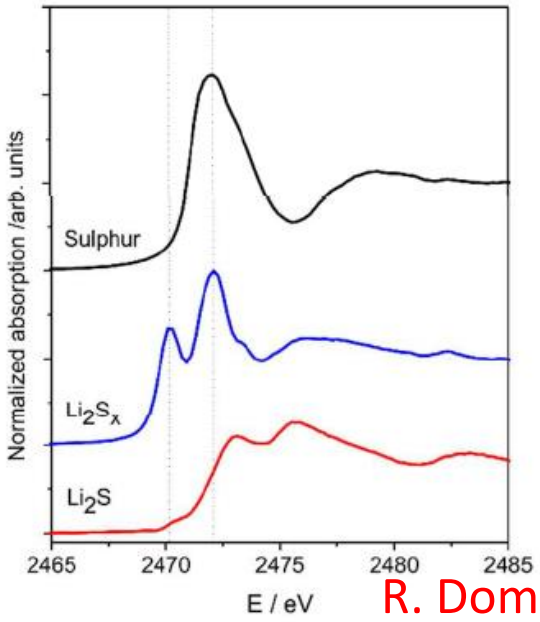

910 min, $Li_{0.76}S$

1933min, $Li_{1.61}S$

R. Dominko et al.(2015)
J. Phys. Chem. C **119**, *19001-19010*

Linear combination fitting

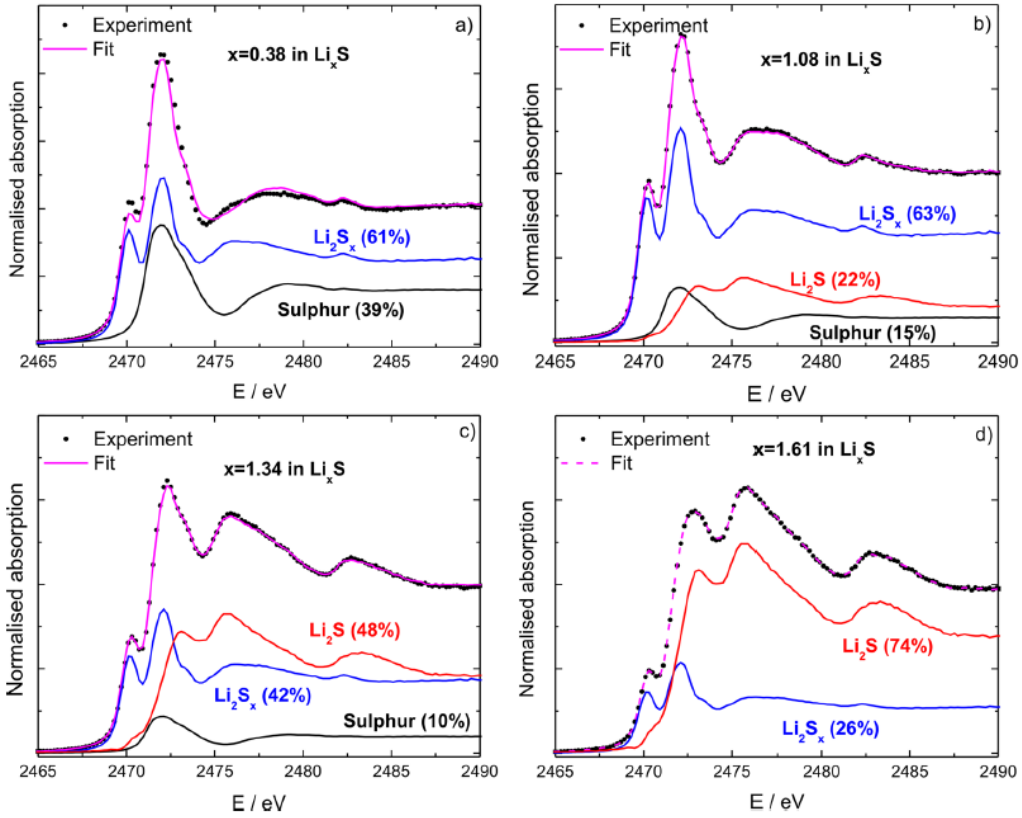

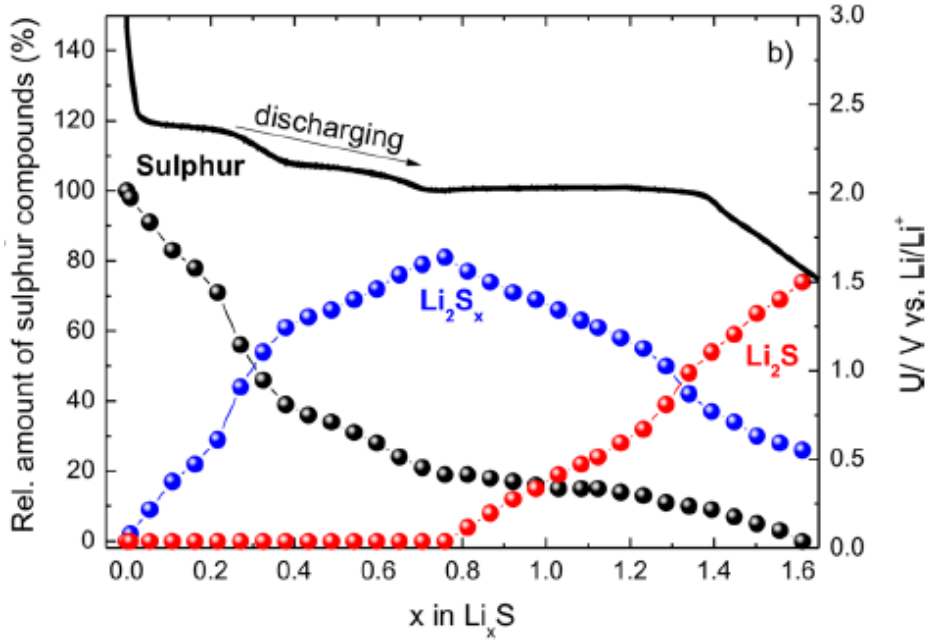

R. Dominko et al.(2015)
J. Phys. Chem. C **119**, *19001-19010*

EXAFS results

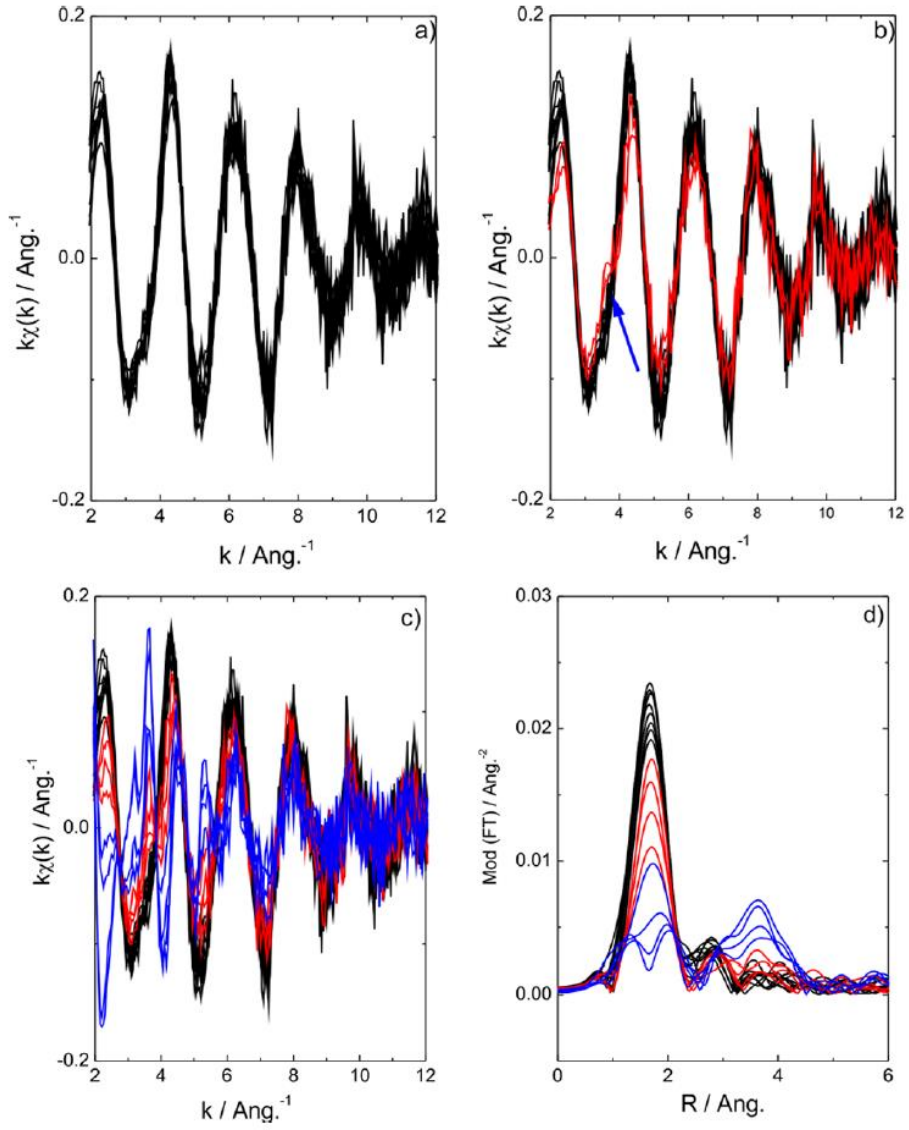

High voltage plateau

- Same main frequency
- Decrease of the intensity
- Compatible with the decrease of the average number of nearest neighbors of sulfur because of the formation of PS

Start of the low voltage plateau

- Appearance of an extra frequency
- Attributed to the onset of the occurrence of Li_2S

R. Dominko et al.(2015)
J. Phys. Chem. C **119**, *19001-19010*

EXAFS results – quantitative analysis

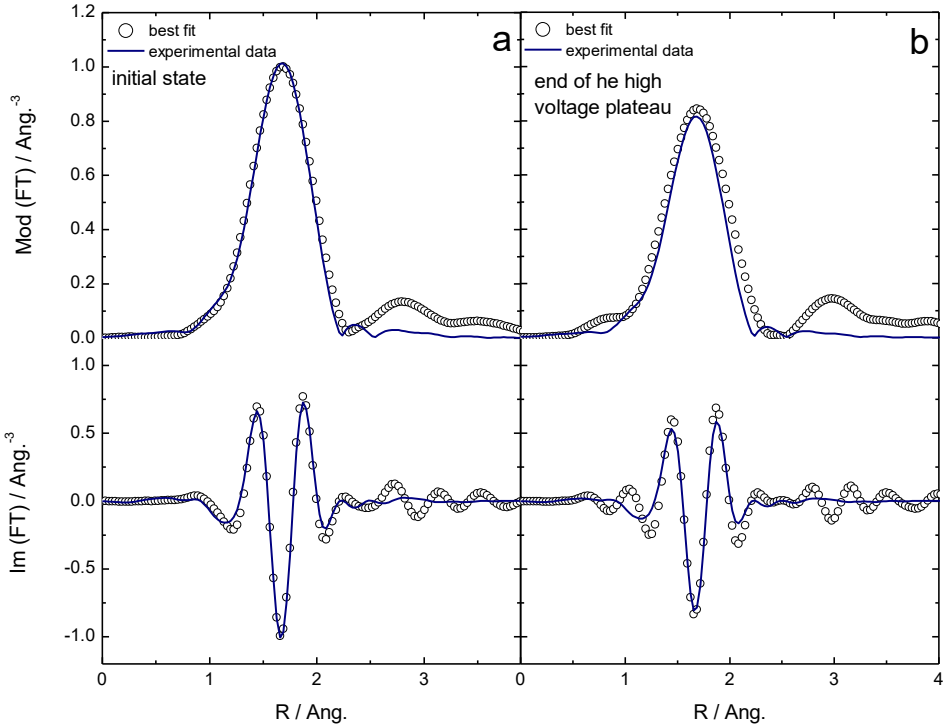

N=2 N=1.6(2)

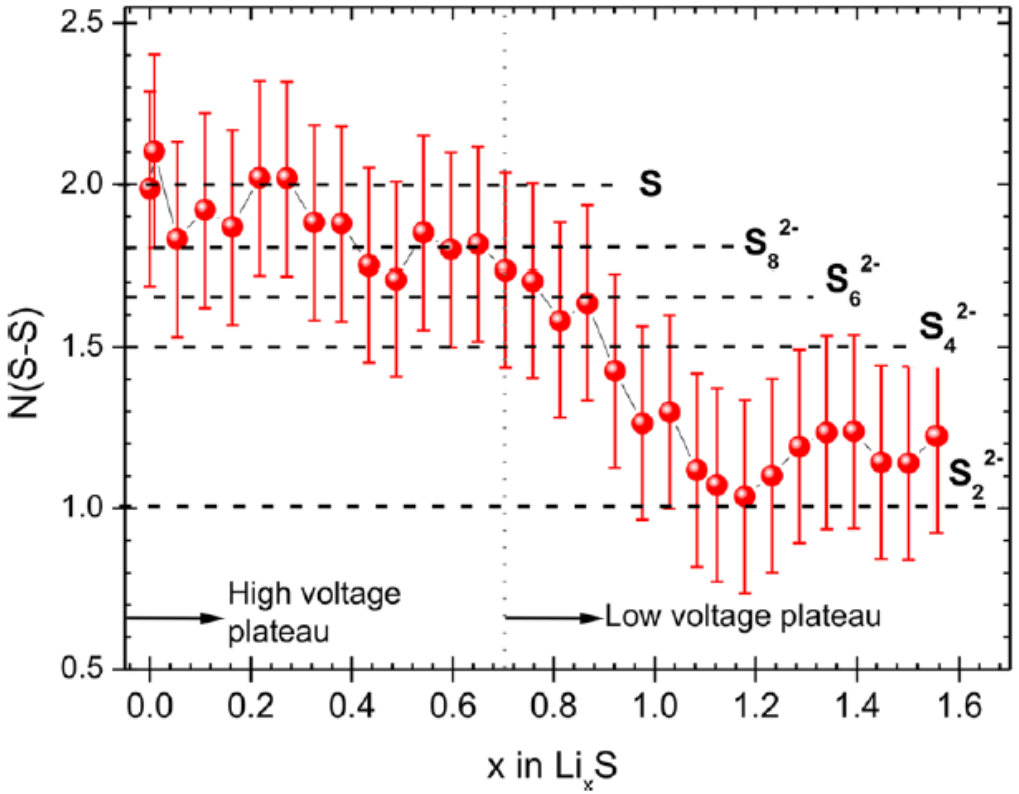

- Sharp decrease of CN at the beginning of the low voltage plateau
- CN constant at the end of the discharge

R. Dominko et al.(2015)
J. Phys. Chem. C **119**, *19001-19010*

Project n. 314515 www.eurolis.eu

Magnetite biomineralization in bacteria - 1

- Many organisms (magnetotactic bacteria) produces magnetic nanoparticles
- Magnetospirillum gryphiswaldense produces magnetite nanoparticles surrounded by a lipidic membrane (magnetosomes)

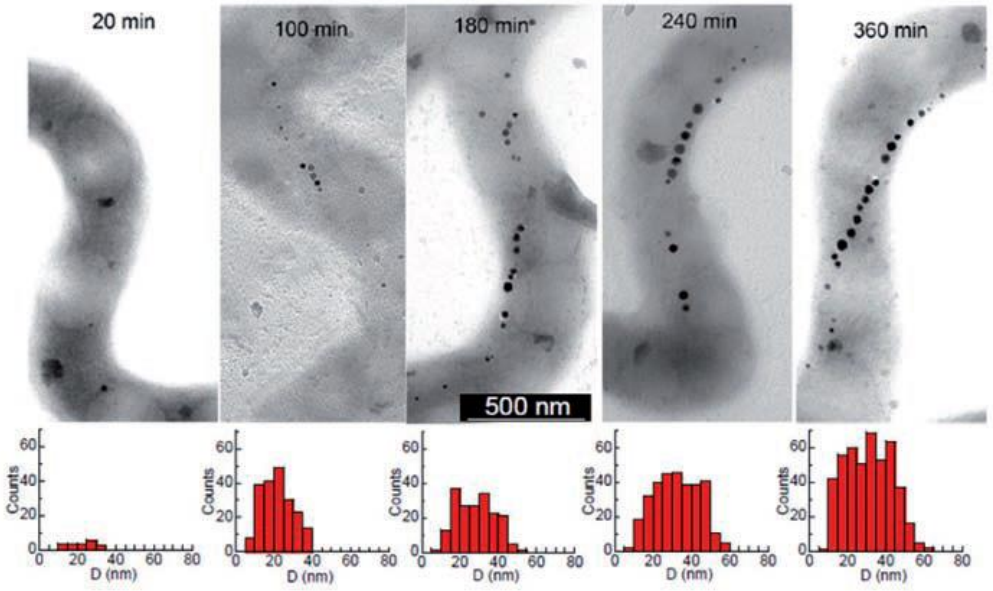

- Chains used as compass needles to orient in the geomagnetic field
- Good biocompatibility and therefore interesting in biomedical applications
- Understanding of the biomineralization process to design new materials

M. L. Fdez Gubieda et al. (2013) *ACS Nano* **7** 3297

Magnetite biomineralization in bacteria - 2

XANES

- To identify the oxidation state and local geometry of the absorbing atom
- To identify and quantify the different Fe phases
- 2 eV shift towards lower energies
- LC of ferrihydrite (Fe^{3+}) and magnetite (Fe^{3+} and Fe^{2+})
- ferrihydrite constant and then in the end of the biomineralization process undetectable

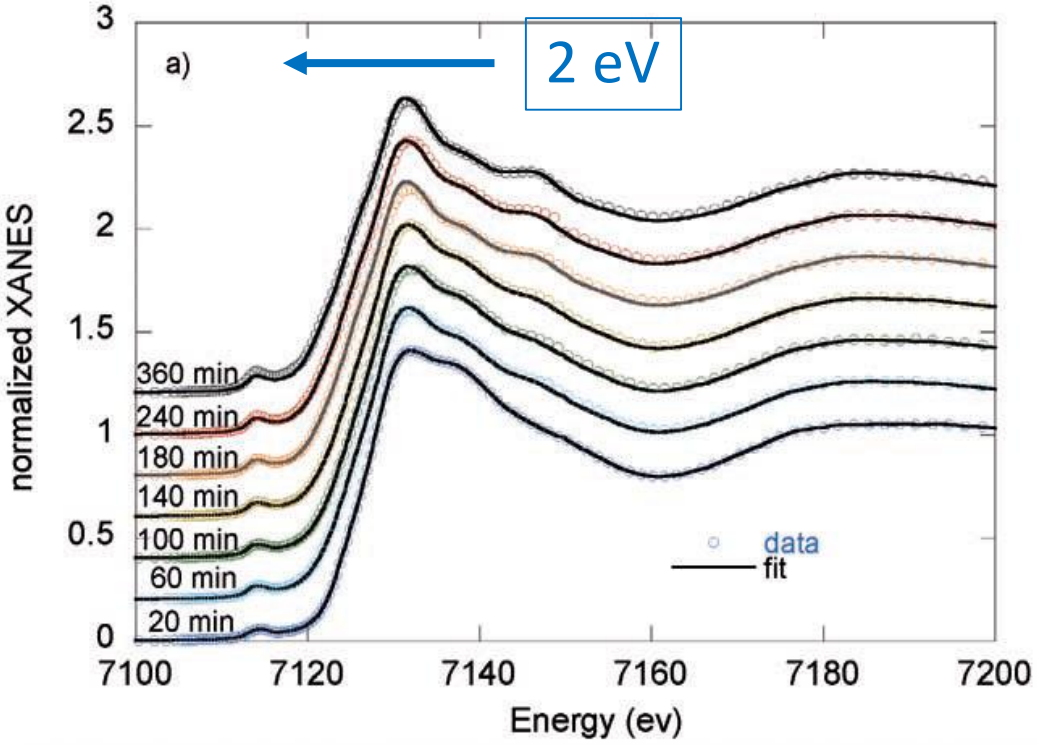

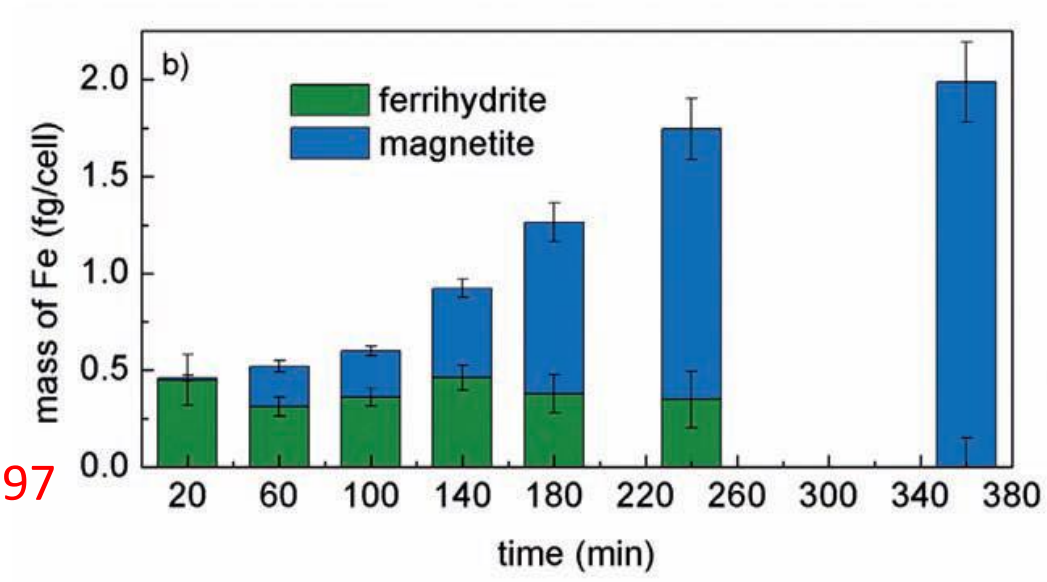

M. L. Fdez Gubieda et al. (2013) *ACS Nano* **7** 3297

Outline

- Energy scanning XAS
  - Operando LiS battery
  - Magnetite biomineralization in bacteria
- **Quick EXAFS**
  - Nucleation of Au NPs
  - Structural kinetics of Pt/C cathode catalyst
- Energy dispersive XAS
  - Magnetism at extreme magnetic fields
  - Photoinduced excited states in complexes
  - Iron melting at high pressure

Quick EXAFS

- Energy scanning
- Time resolution down to ms (~ 100 Hz oscillations)
- Double crystal monochromator: grooved channel cut
  - Rotation is the only movement
  - Both diffracting parts are naturally aligned

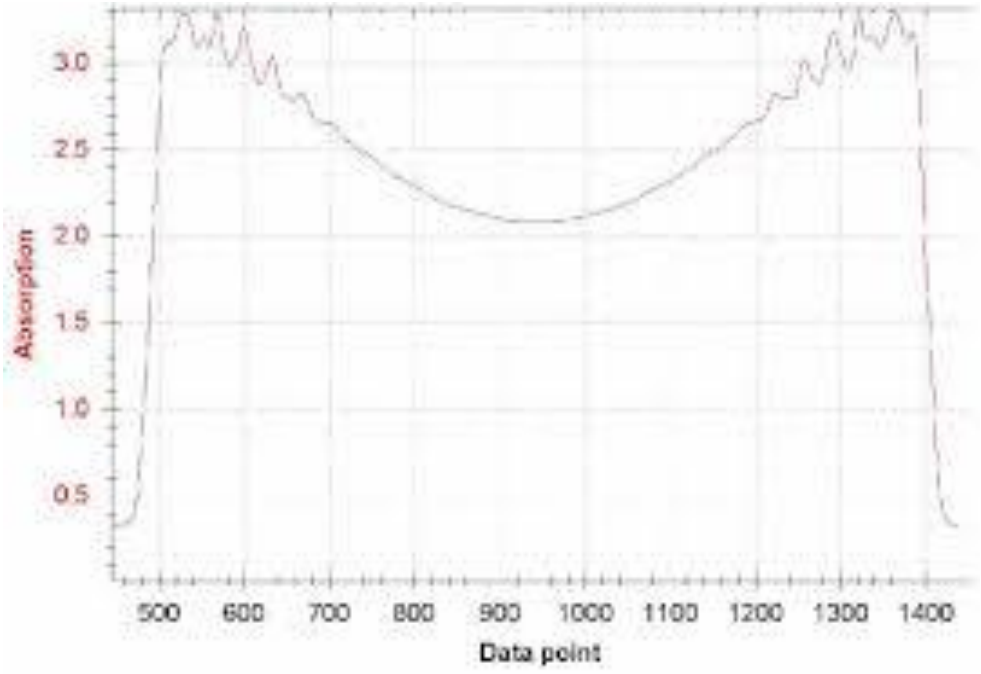

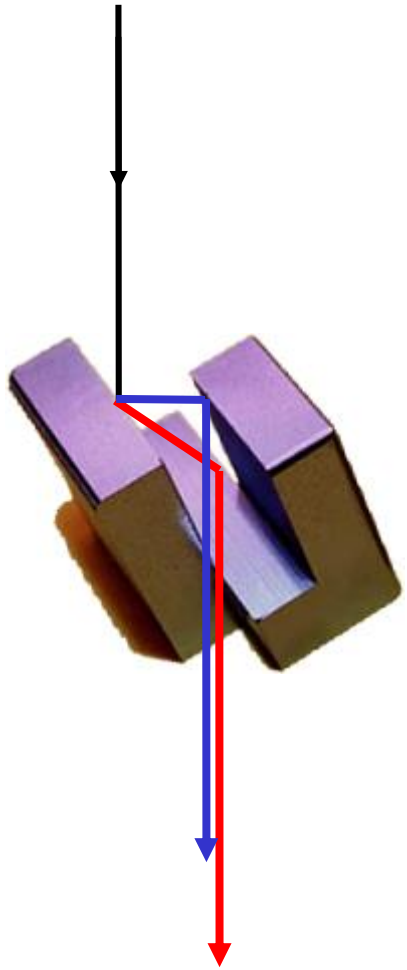

Nucleation of Au NPs by QEXAFS spectroscopy

- Au NPs have unique properties in the fields of electronics, magnetics, optics and catalysis
- The unique properties of Au NPs can be controlled by controlling their size and shape
- Au NPs can be synthesized easily by the reduction of Au^{3+} ions in a solution containing protective agents
- Despite its importance, the formation process of Au NPs is still unclear.
- This is because there are only a few effective techniques for *in situ* observations.

N. Ohyama et al. (2011) *ChemPhysChem* **12**, 127-131

Nucleation of Au NPs by QEXAFS spectroscopy

Experiment

- Measurements at Spring-8
- $HAuCl_4$ in toluene with dodecanthiol
- DMF solution of $NaBH_4$
- 100 ms time resolution
- After the addition of the reducing agent, reaction monitored for 180 seconds

N. Ohyama et al. (2011) *ChemPhysChem* **12**, 127-131

Nucleation of Au NPs by QEXAFS spectroscopy

Elettra Sincrotrone Trieste

Evolution before the reducing agent

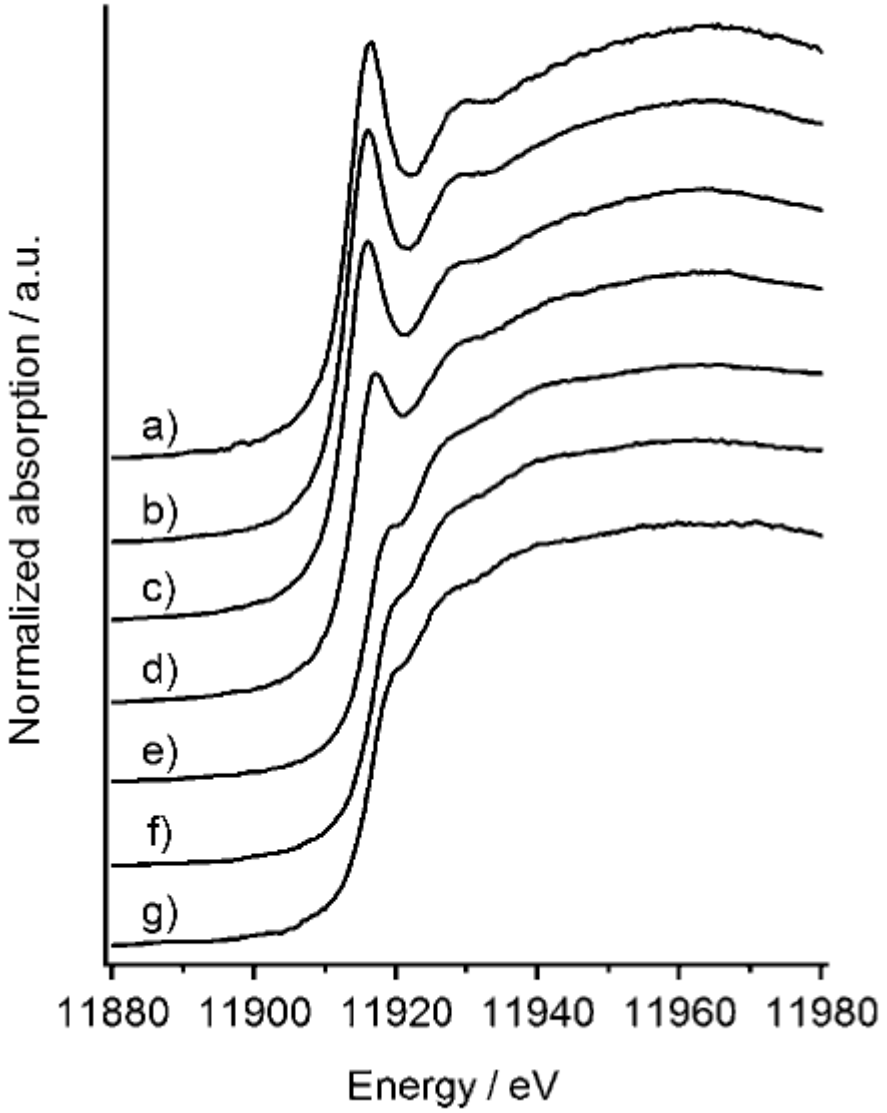

$DT/HAuCl_4 = 0$
$DT/HAuCl_4 = 0.1$
$DT/HAuCl_4 = 0.4$
$DT/HAuCl_4 = 1$
$DT/HAuCl_4 = 2$
$DT/HAuCl_4 = 4$
$DT/HAuCl_4 = 16$

Table 1. The fractions of Au^{3+} and Au^{+} in the solution with various DT/Au ratios before $NaBH_4$ reduction. The fractions were evaluated by fitting of the XANES spectra of various DT/Au with linear combination of those of DT/Au = 0 and 16.

DT/Au	0.1	0.4	1	2	4
Au^{3+} [%]	90.3	79.0	50.3	0	0
Au^{+} [%]	9.7	21.0	49.7	100	100
R factor	0.006	0.004	0.005	0.009	0.007

N. Ohyama et al. (2011) *ChemPhysChem* **12**, 127-131

Nucleation of Au NPs by QEXAFS spectroscopy

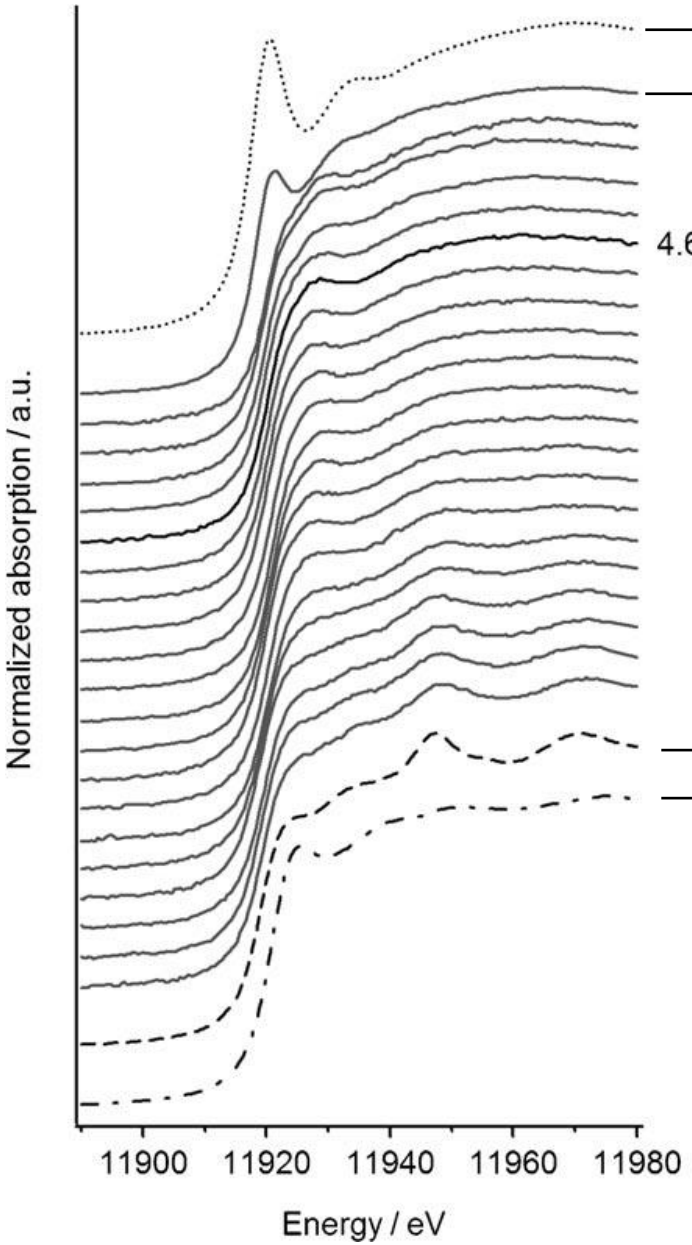

$HAuCl_4$ in Toluene

$HAuCl_4$ in DT (ratio=1)

Au

$Au_{11}(PPh_3)_8Cl_3$

N. Ohyama et al. (2011) *ChemPhysChem* **12**, 127-131

Nucleation of Au NPs by QEXAFS spectroscopy

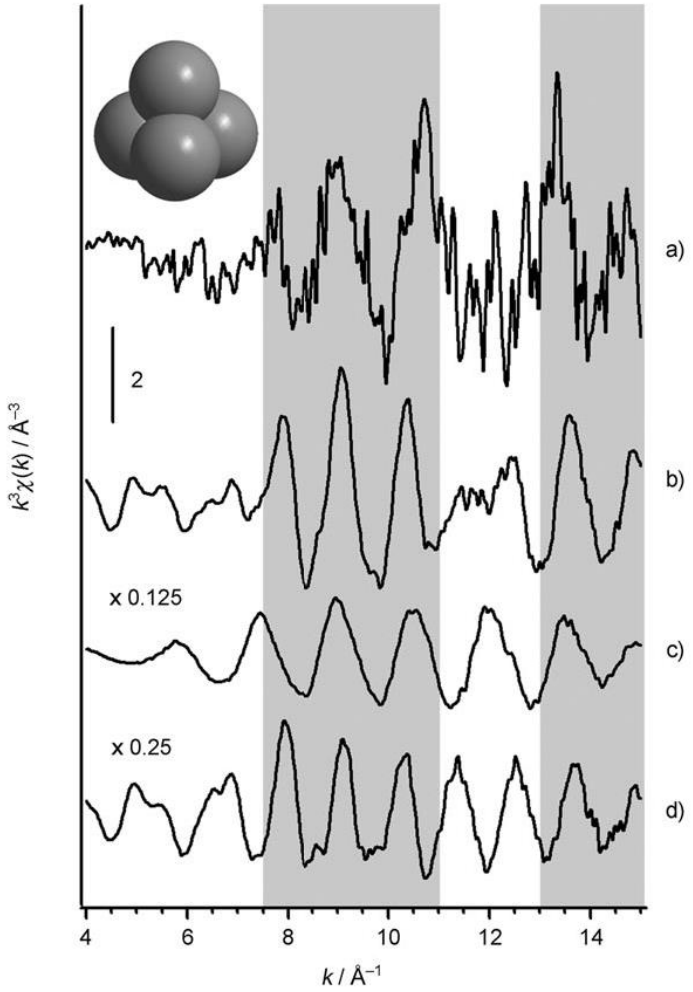

→ t = 4.6 s

→ $HAuCl_4$ in DT (ratio=1)

→ Au

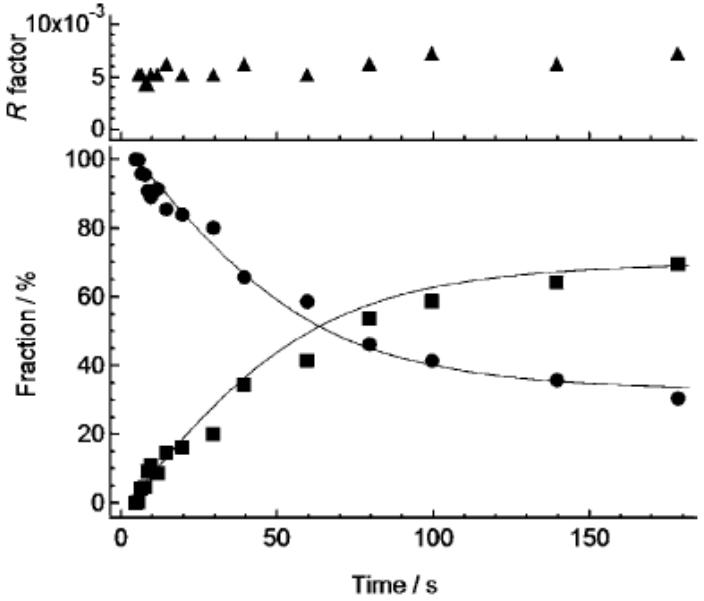

N. Ohyama et al. (2011) *ChemPhysChem* **12**, 127-131

Structural kinetics of Pt/C cathode catalyst

The understanding of the structural and electronic properties of the catalytic active site during the catalytic activity is of prime significance to obtain a rational catalyst design that points towards the improvement of already established reaction and to develop catalyst for new reactions.

(a) 0.4 V (under N_2)
(b) 1.0 V (under N_2)

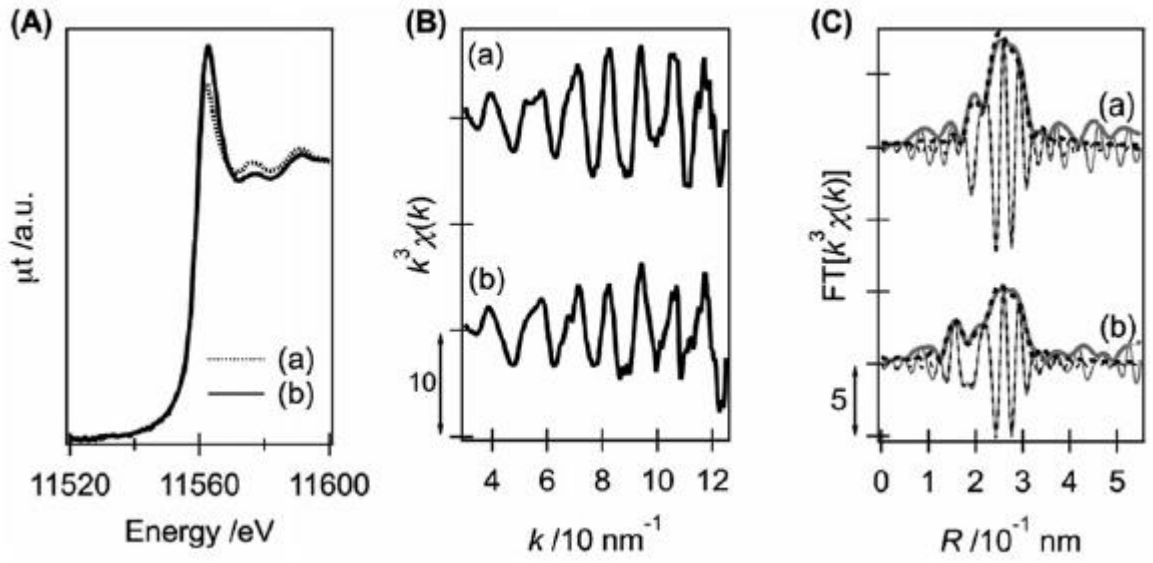

N. Ishiguro et al. (2013) *Phys.Chem.Chem.Phys.* **15**, 18827

Structural kinetics of Pt/C cathode catalyst

0.4 V → 1 V (under N_2)

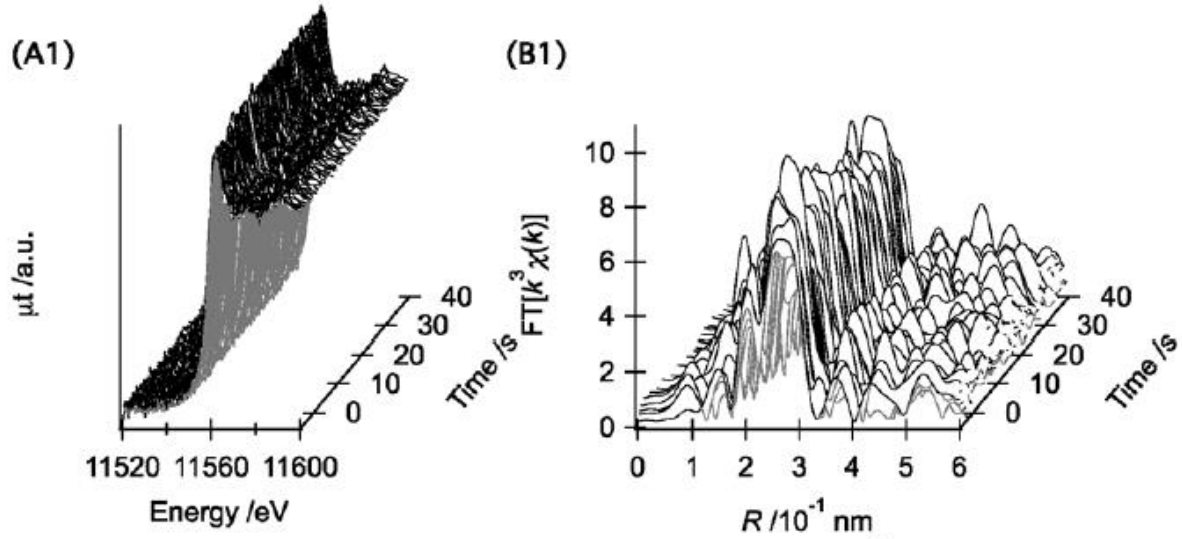

1 V → 0.4 V (under N_2)

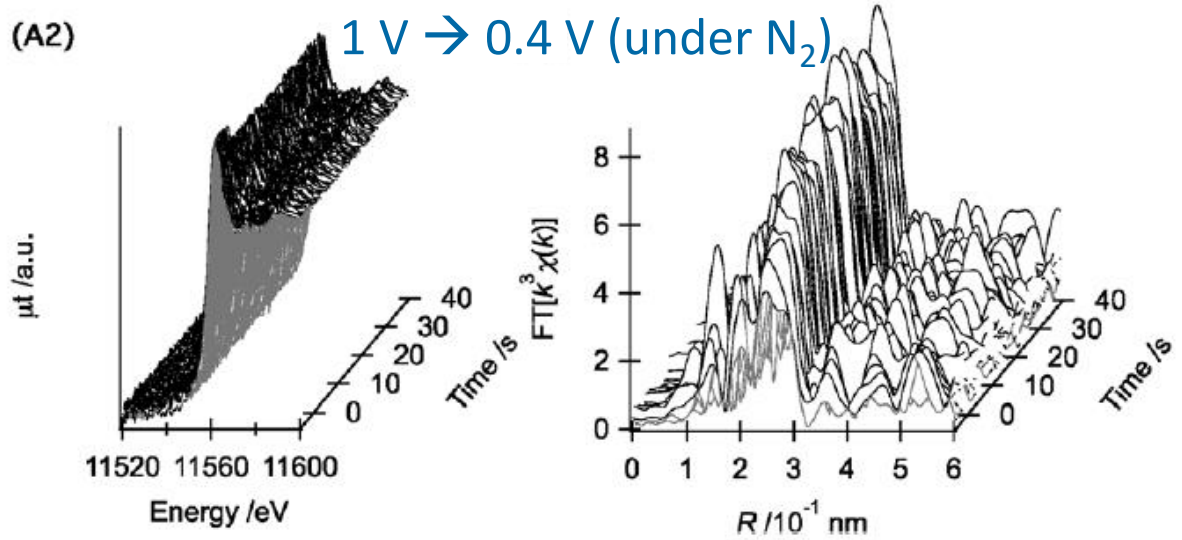

N. Ishiguro et al. (2013) *Phys.Chem.Chem.Phys.* **15**, 18827

giuliana.aquilanti@elettra.eu

Elettra Sincrotrone Trieste

Structural kinetics of Pt/C cathode catalyst

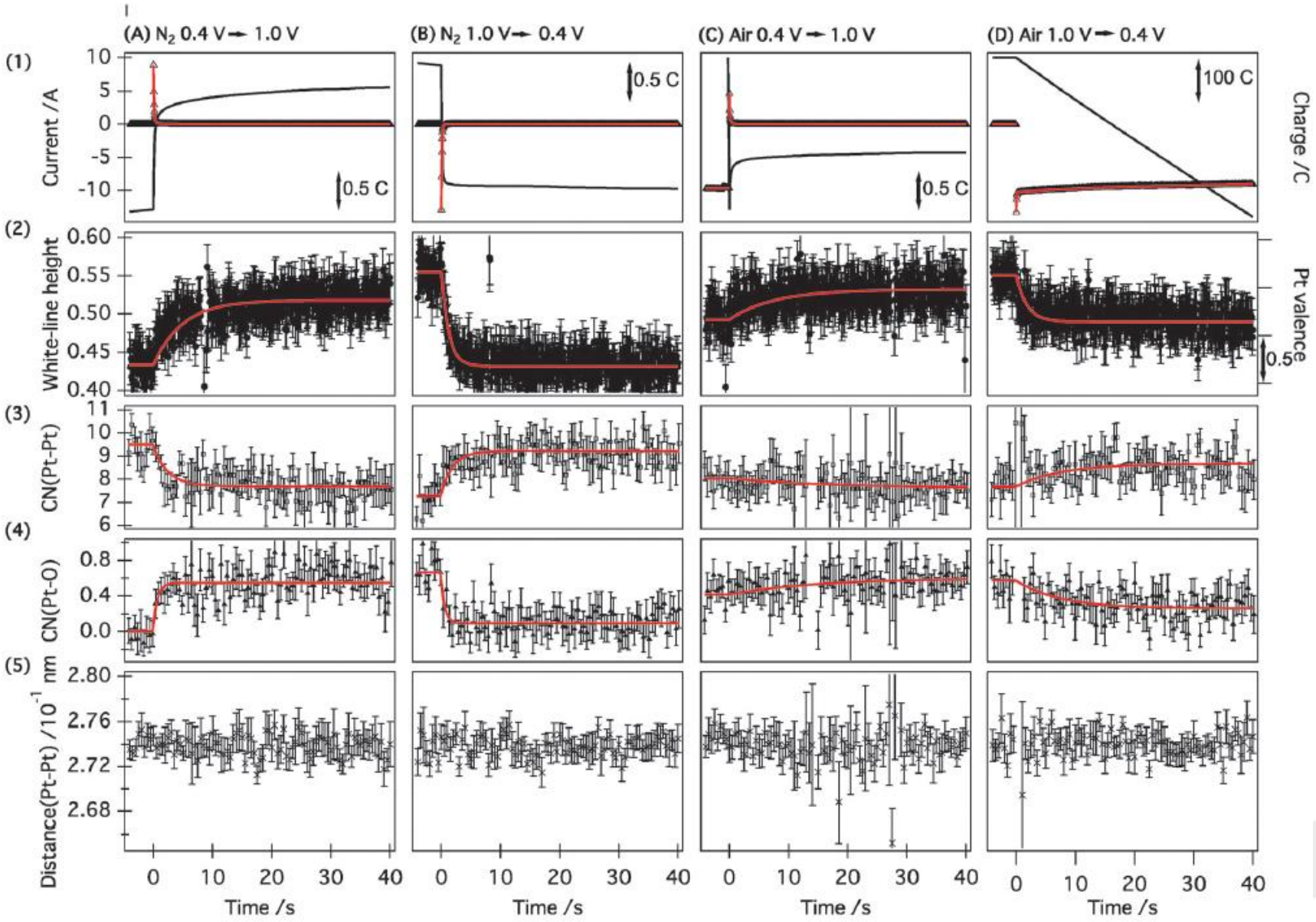

N. Ishiguro et al. (2013) *Phys.Chem.Chem.Phys.* **15**, 18827

giuliana.aquilanti@elettra.eu

Structural kinetics of Pt/C cathode catalyst

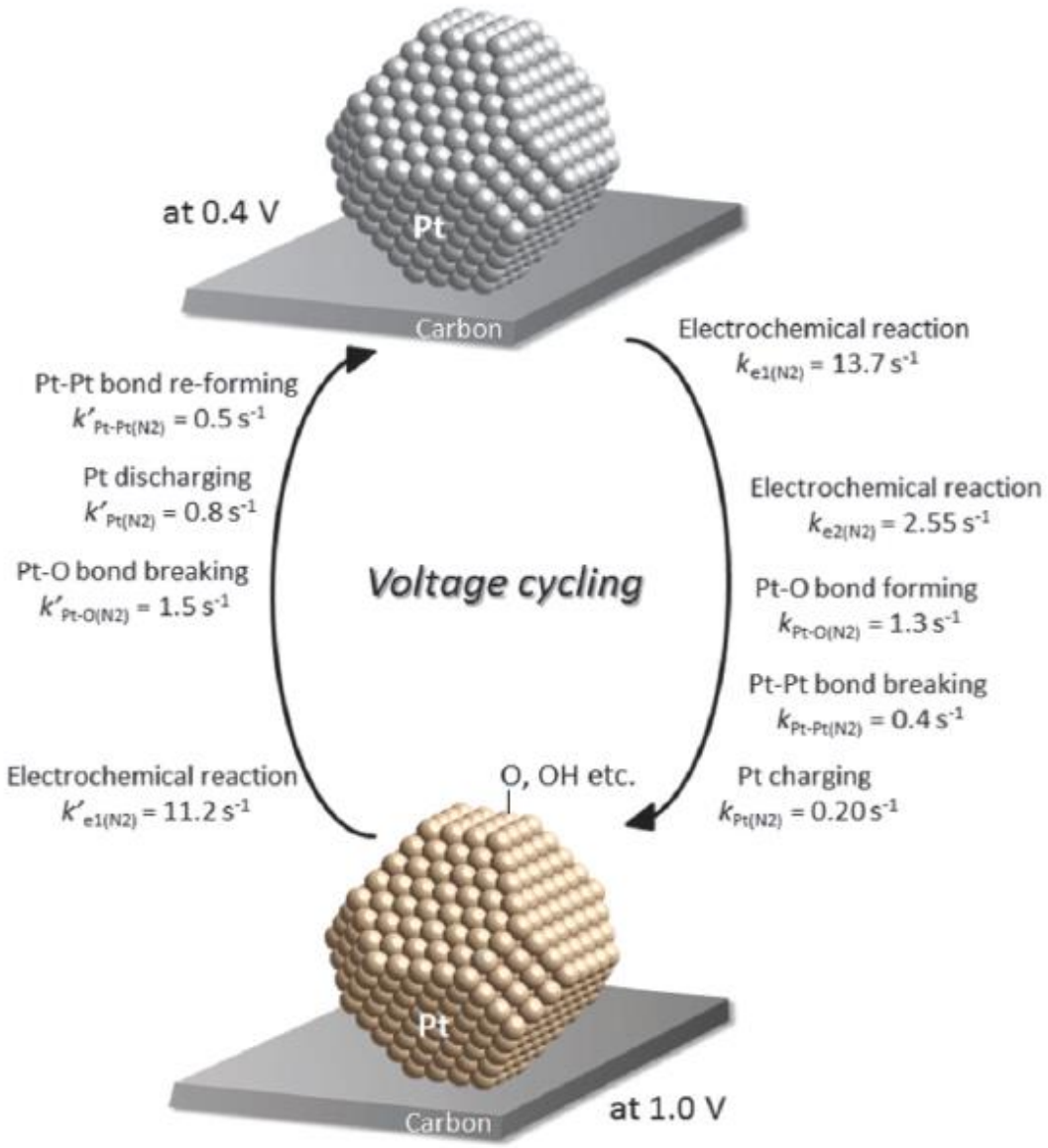

N. Ishiguro et al. (2013) *Phys.Chem.Chem.Phys.* **15**, 18827

Elettra Sincrotrone Trieste

Outline

- Energy scanning XAS
  - Operando LiS battery
  - Magnetite biomineralization in bacteria
- Quick EXAFS
  - Nucleation of Au NPs
  - Structural kinetics of Pt/C cathode catalyst
- **Energy dispersive XAS**
  - Magnetism at extreme magnetic fields
  - Photoinduced excited states in complexes
  - Iron melting at high pressure

Energy dispersive EXAFS

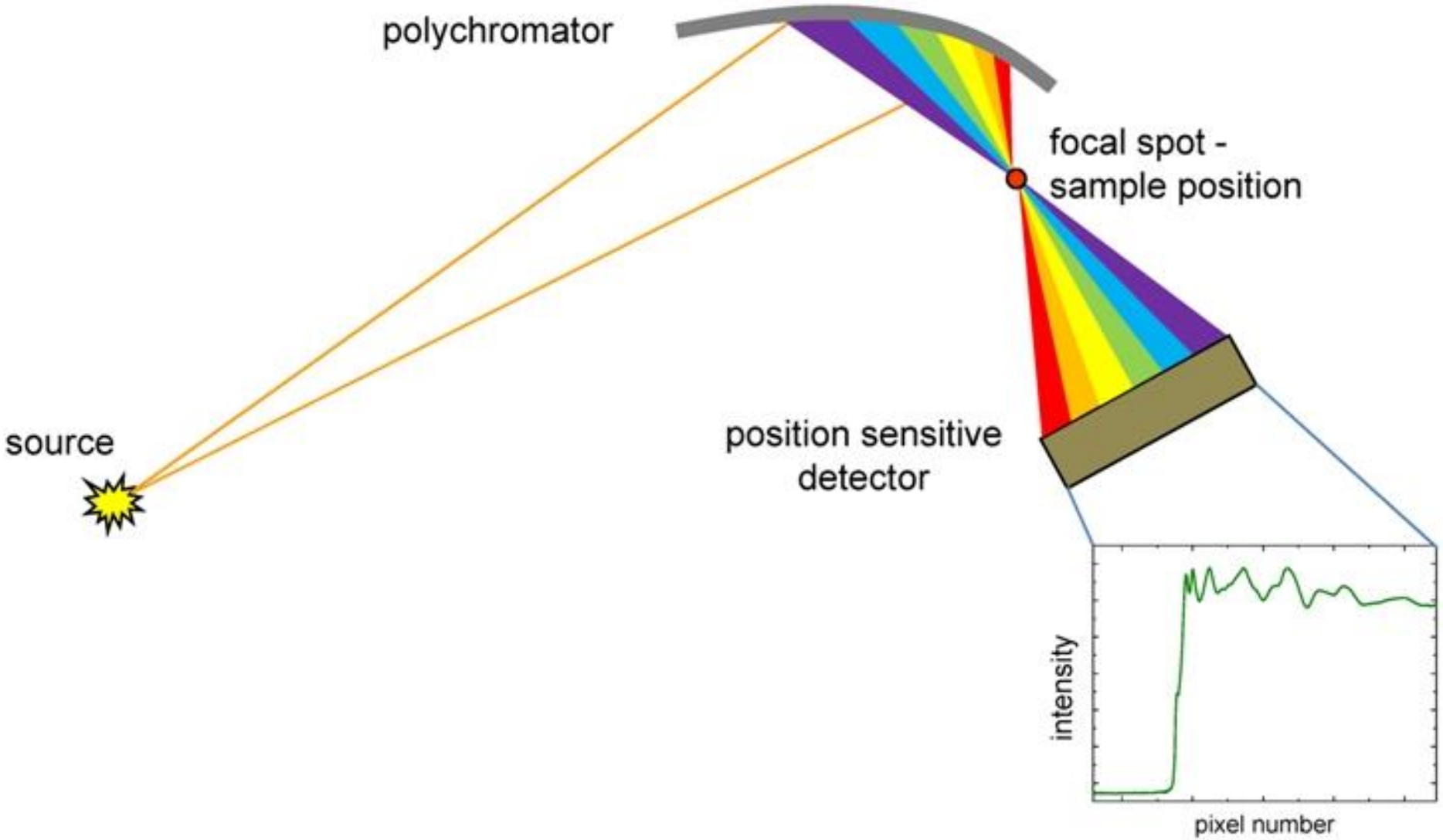

Elettra Sincrotrone Trieste

EDXAS

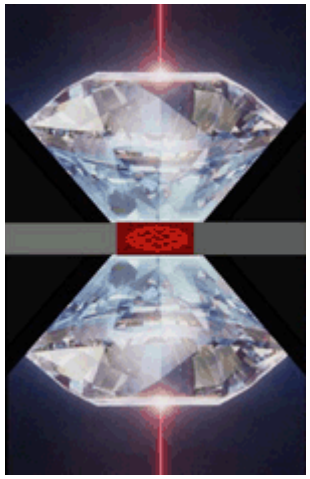

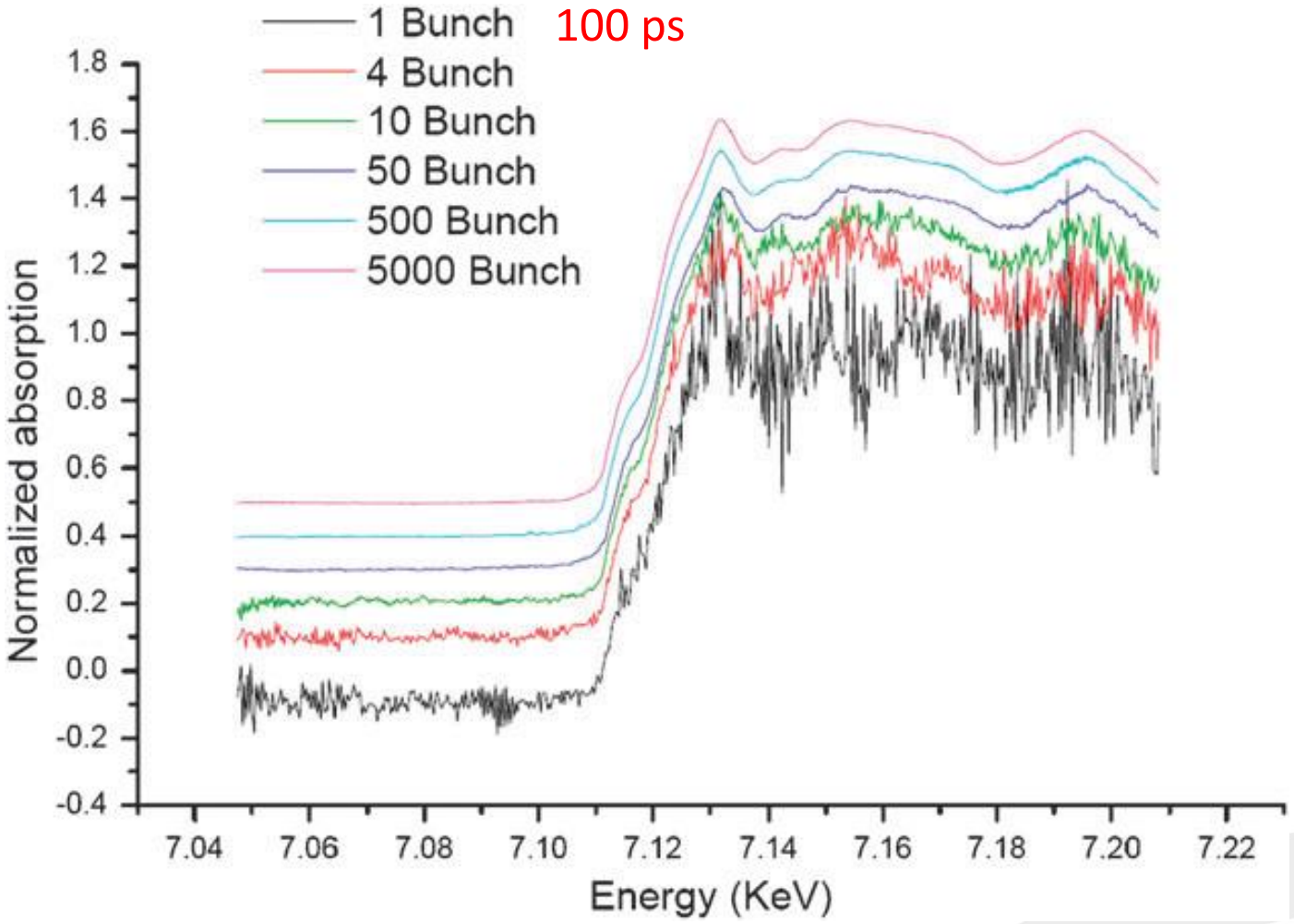

Pascarelli et al. (2010) *Phys.Chem.Chem.Phys* **12**, 5535

Elettra Sincrotrone Trieste

Scanning vs. energy dispersive

	Energy Scanning	Energy Dispersive
stability	mechanical movement	no movement of optics during acquisition
speed	energy points acquired sequentially	all energy points acquired simultaneously
optical scheme	simple	less simple
detection de-excitation channels (XRF, XES, RIXS)	straightforward	flux-energy resolution tradeoff
demands on sample microstruct	low	high
focal spot min	50-100 nm	2-3 μm
pump-probe	ps/energy point	ps/full spectrum
single shot	50 - 100 ms/spectrum	1 μs/spectrum at 3rd gen

From S. Pascarelli, smr2332 (2012)

Magnetism at extreme magnetic field

Extreme conditions

- High pressure (multimegabar with DACs)
- High temperature (thousands of K with laser heating)
- Low temperatures (millikelvin with diluition refrigerators)

⇩

New phenomena

High magnetic fields

- Structural and magnetic phase transition
- Discovery of previously unexplored quantum critical points

Typical values:

- 60 T
- Time duration: 0.1-50 ms

Characterization of electronically excited states of Cu(I) complexes

- Photoinduced excited state of two Cu(I) complexes: $[Cu(dmp)_2]^+$, $[Cu(dbtmp)_2]^+$
- EDXAS (ID24- ESRF)
- Very fast detector (Ge microstrip) gated around a single bunch (100 ps) of synchrotron light
- Excitation with 450 nm laser with 10 Hz repetition
- MLCT states
- Excited states monitored for up to 100 ns

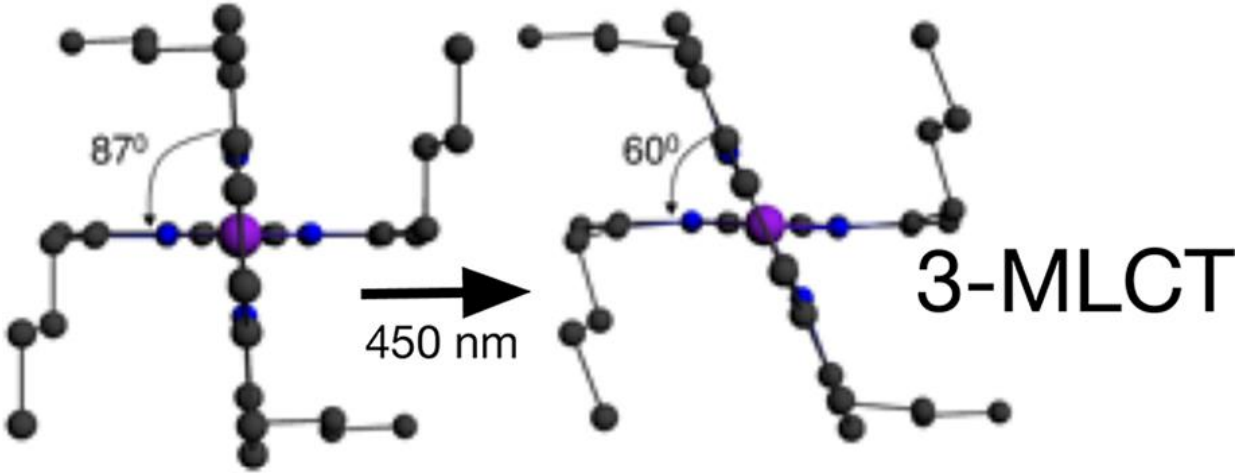

Tromp et al. (2013) *J. Phys. Chem B* **117**, 7381

Characterization of electronically excited states of Cu(I) complexes

- Photoexcitation of molecules has applications in solar energy, conversion and storage, chemical sensing , photocatalysis
- $[Cu(dmp)_2]^+$ (2,9-dimethyl-1,10-phenantrolyne)

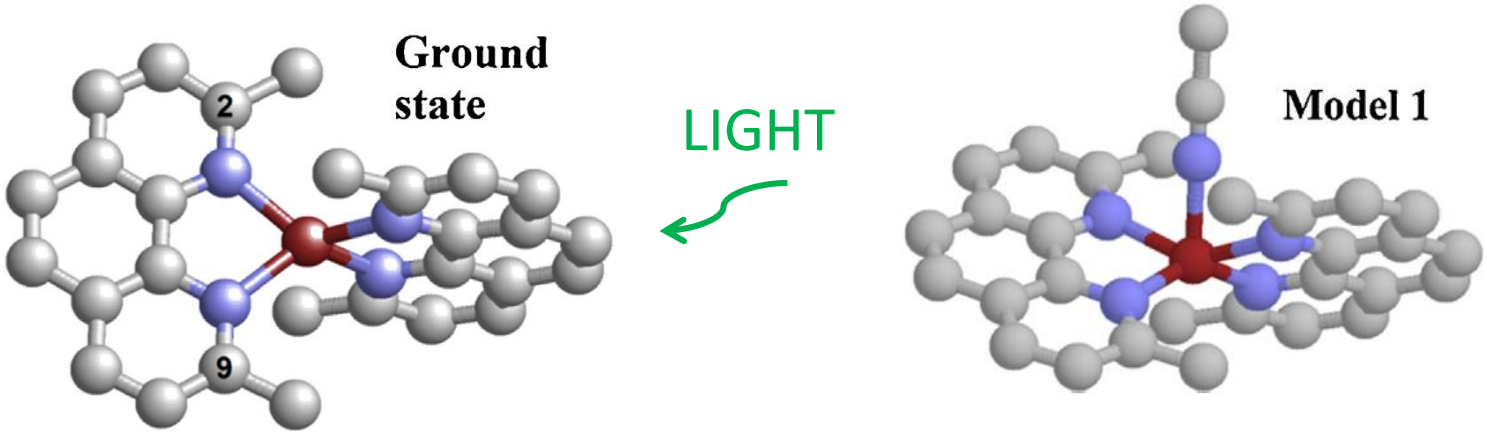

d^{10} configuration
distorted tetrahedral geometry

MLCT excited state with a Cu^{II*} center
flattened geometry

- The large shift observed between absorption and photoluminescence is consistent with significant structural changes in the MLCT excited state
- The decay to the ground state happens via a radiative decay pathway or forms a pentacoordinate complex resulting in exciplex quenching in the ligated MLCT state

Tromp et al. (2013) *J. Phys. Chem B* **117**, 7381

Characterization of electronically excited states of Cu(I) complexes

- Up until a few years ago, structural information on the MLCT state of [CuI(dmp)2]+ was mostly indirect.
- In the last 10 years time-resolved X-ray techniques based on XAS have been used to study these Cu(I) systems and confirm the formation of an exciplex providing direct evidence for a five-coordinated species

Energy scanning XAS for a total time of 40 h!

Tromp et al. (2013) *J. Phys. Chem B* **117**, 7381

Characterization of electronically excited states of Cu(I) complexes

Pump and probe EDXAS experiment

- 10 Hz Quantel Brilliant Q-Switched Nd:YAG laser,
  - Pulse width: 3ns
  - Laser excitation: 450 nm
  - 12 mJ per pulse

PUMP

- ID24 beamline (ESRF)
- 4-bunch mode
  - 10^7 photons per single bunch in the bandwidth used
  - Pulse duration: 100 ps
  - Interval between bunches: 700 ns

PROBE

- Ge microstrip detector (XH)
  - rapid enough in its acquisition time to isolate an individual electron bunch
  - time-windowed (500 ns integration time) around the electron bunch
  - 100 kHz repetition rate

DETECTION

Tromp et al. (2013) *J. Phys. Chem B* **117**, 7381

giuliana.aquilanti@elettra.eu

Characterization of electronically excited states of Cu(I) complexes

Pump and probe EDXAS experiment

- The ESRF machine clock signal (352.2 MHz) was used as a timing basis to trigger the XH detector, and the flashlamp and Q-switch of the laser to vary the delay between excitation and recording
- X-ray spot: 5 μm x 100 μm perpendicular to the laser excitation
- Alternating light-on and light-off measurements were be taken providing direct XAS difference-spectra

Energy dispersive XAS for a total time of 2 h!

Tromp et al. (2013) *J. Phys. Chem B* **117**, 7381

Characterization of electronically excited states of Cu(I) complexes

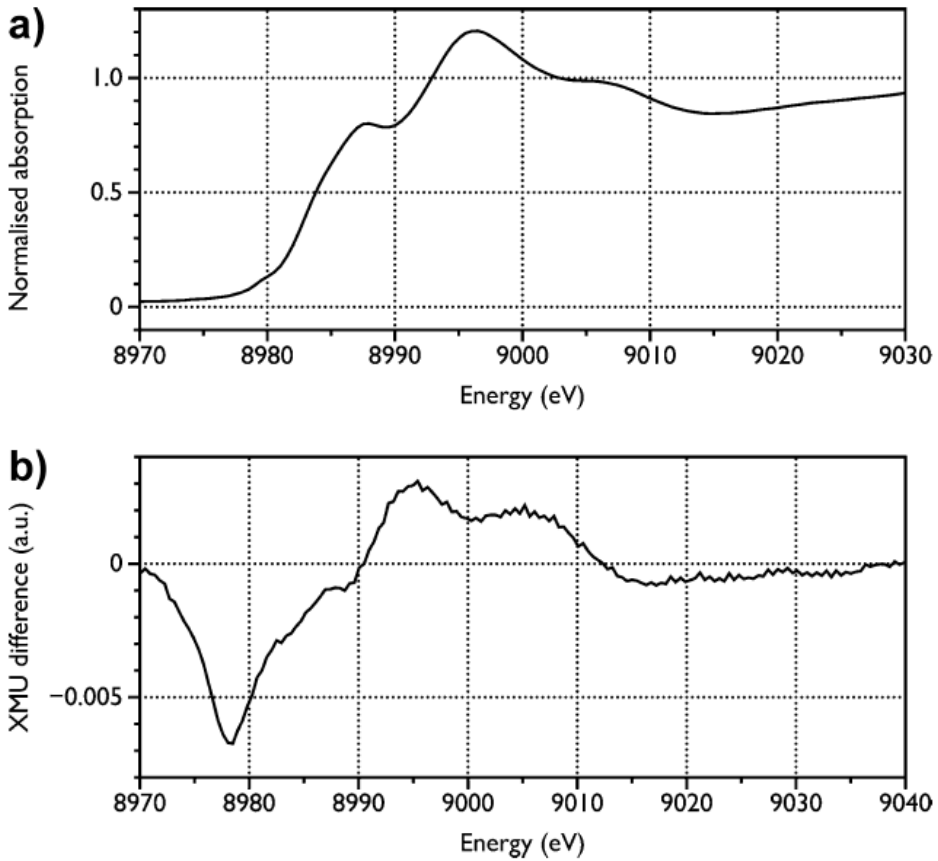

Spectrum of the ground state of $[Cu(dmp)_2]^+$ in acetonitrile

XANES difference spectrum before (-5 ns) and after excitation (+5 ns)

Tromp et al. (2013) *J. Phys. Chem B* **117**, 7381

giuliana.aquilanti@elettra.eu

Characterization of electronically excited states of Cu(I) complexes

XANES calculations

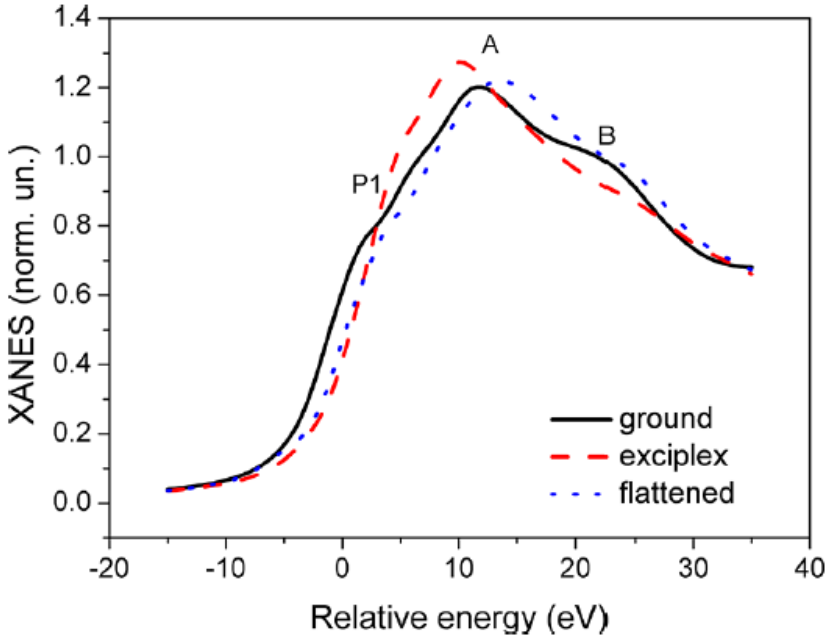

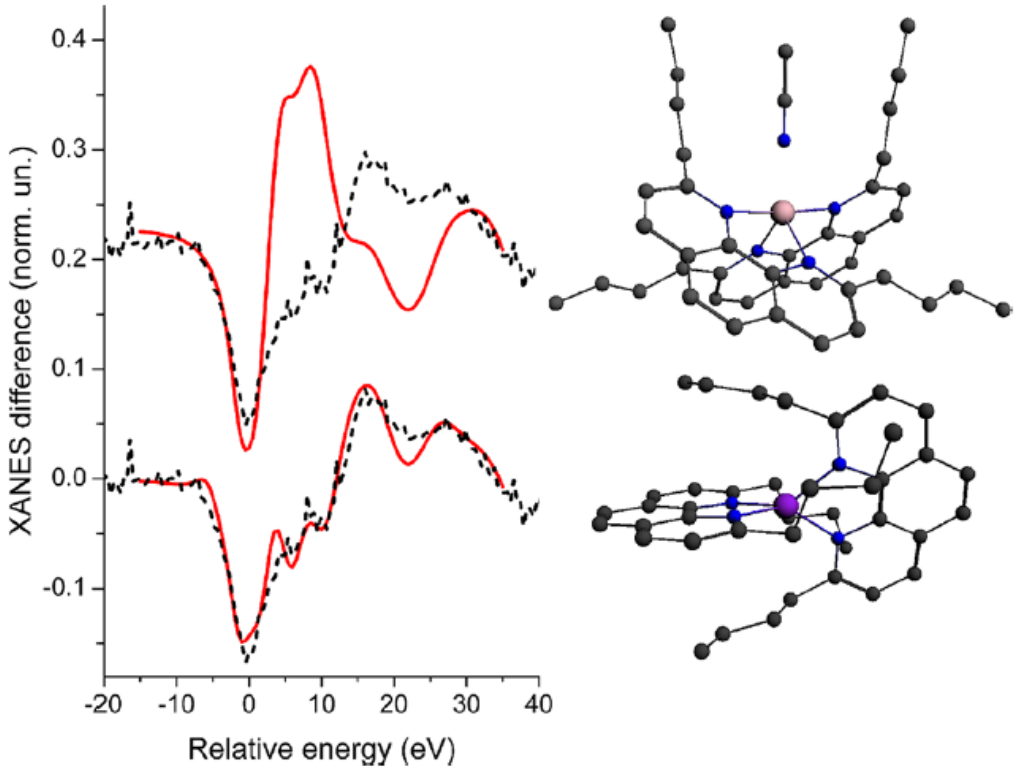

Tromp et al. (2013) *J. Phys. Chem B* **117**, 7381

Melting of iron determined by EDE

- Fe is the principal component of the Earth's core
- The knowledge of the melting curve is a major concern in geophysics
- The melting temperature of iron at ICB (330 GPa) constraints the thermal gradient and thus the heat fluxes
- This is fundamental to understand the Earth's dynamo and its implications to the terrestrial magnetic field
- Discrepancies as large as 2000 K at the ICB (800 K at 100 GPa)

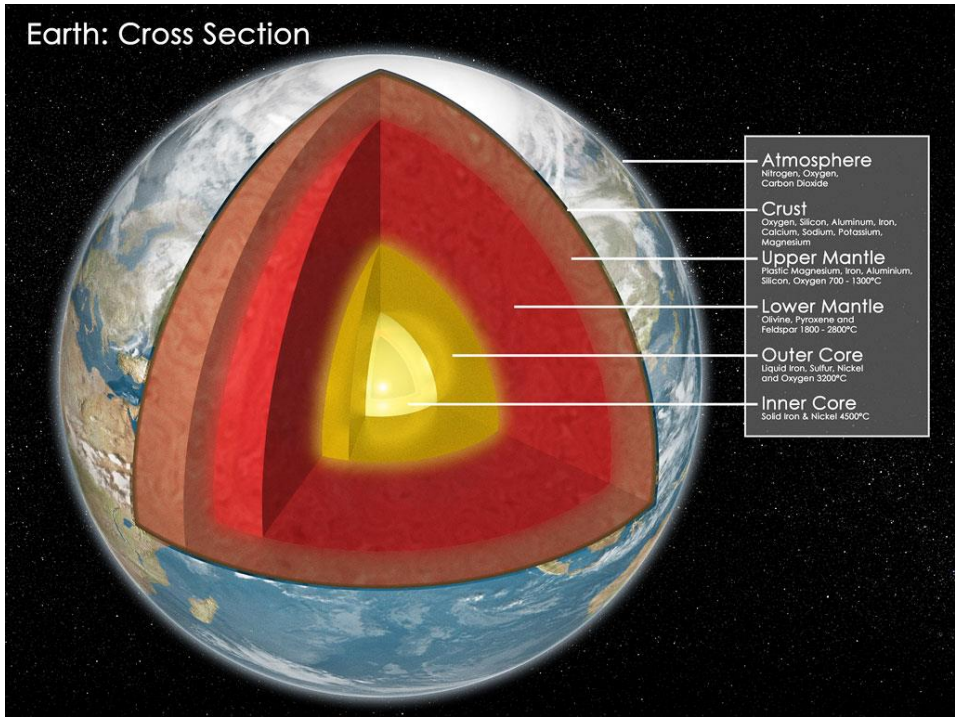

giuliana.aquilanti@elettra.eu

Melting of iron determined by XAS (XANES)

- XAS maintains the same accuracy and sensitivity regardless the physical state of the investigated sample
- Similarly to diffraction techniques, XANES may distinguish different crystallographic phases, but gives in addition information on electronic structure
- The XANES spectra contain solely the signal relative to the absorbing element, without any interference of the container or experimental environment

giuliana.aquilanti@elettra.eu

Sample preparation

- The sample container consists of two sapphire plates manufactured using a combination of micro polishing and focused ion beam milling
- The cavity dimension: 18 µm diameter and 6 µm depth

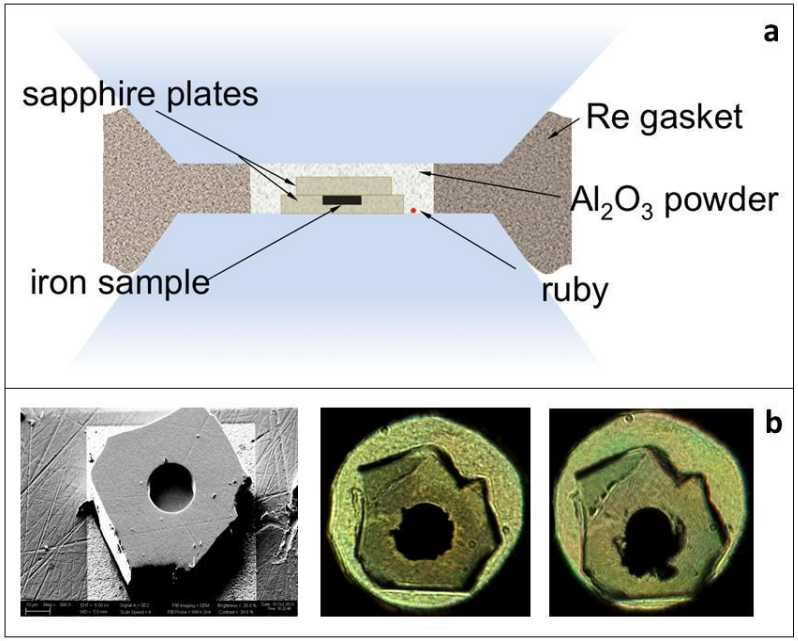

- All is embedded in a very fine grained Al2O3 powder which molds around the capsule to prevent fracture during loading and after laser heating

Samples at melting

- Unstable sample at melting

Dewaele et al. (2007) *PRB* **76**, 144106

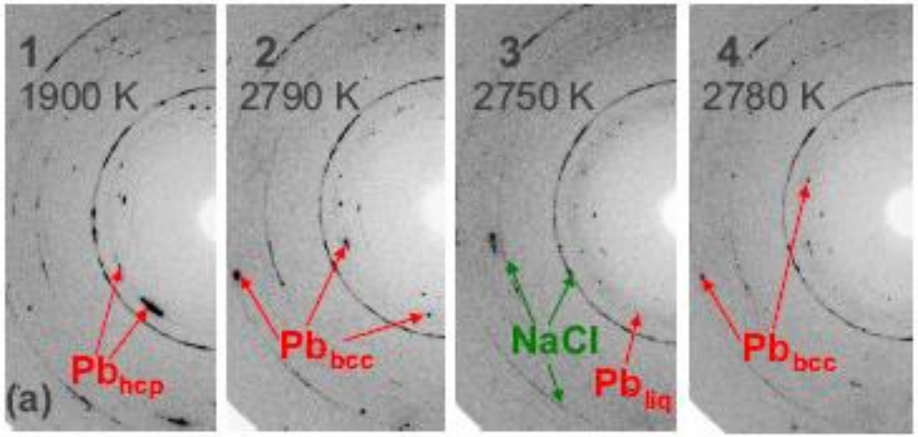

- Melting of lead
- Rapid crystallization of the sample just before the diffuse ring appearance which could only be recorded for few seconds

XANES measurements at ID24 (ESRF)

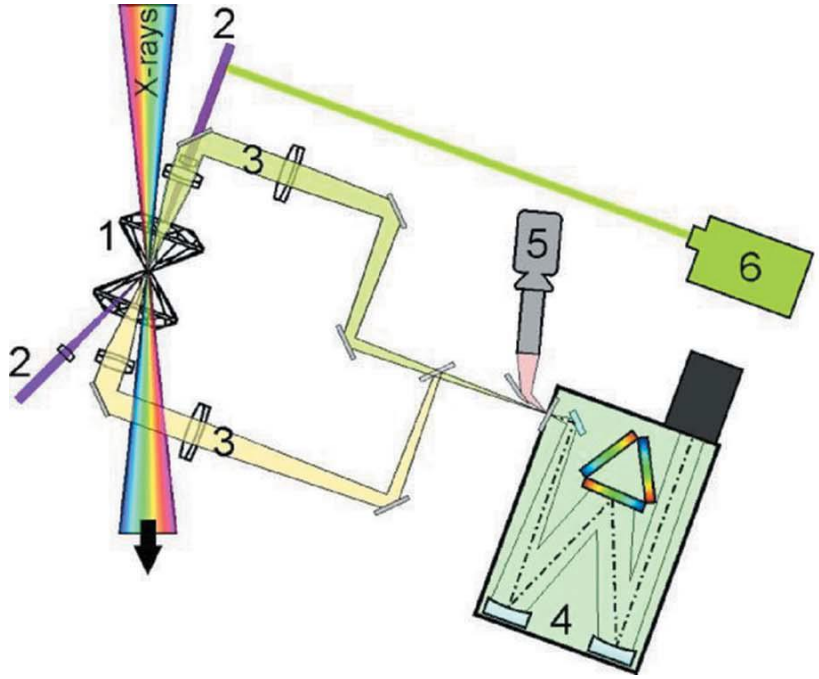

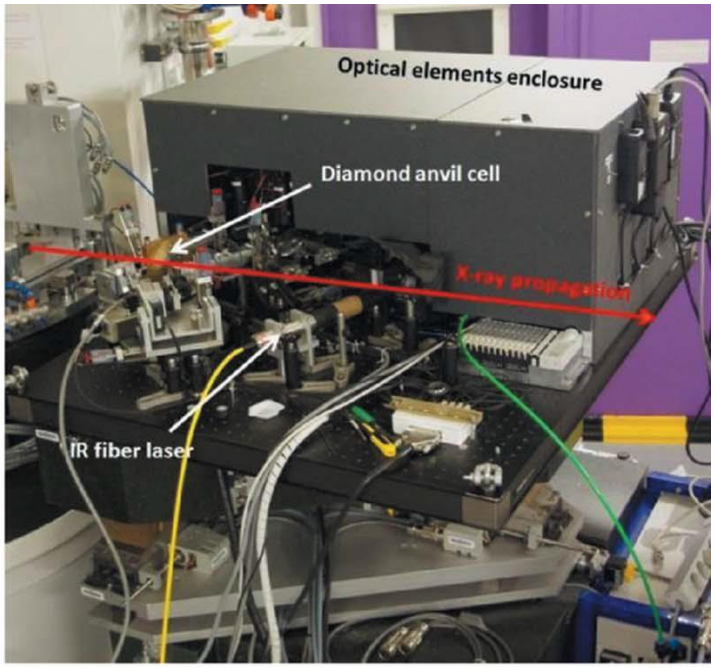

Pascarelli et al. (2016) *J. Synch. Rad* **23**, 23353

- X-ray beam size: 5 x 5 μm^2
- XANES spectra collected every few seconds before, during and after heating
- Four different runs from 63 to 103 GPa and temperatures up to 3530 K
- For each heating cycle, the laser power is ramped up incrementally and kept constant for several seconds to record the XAS spectrum and light emission to measure the temperature.

hcp to fcc phase transition

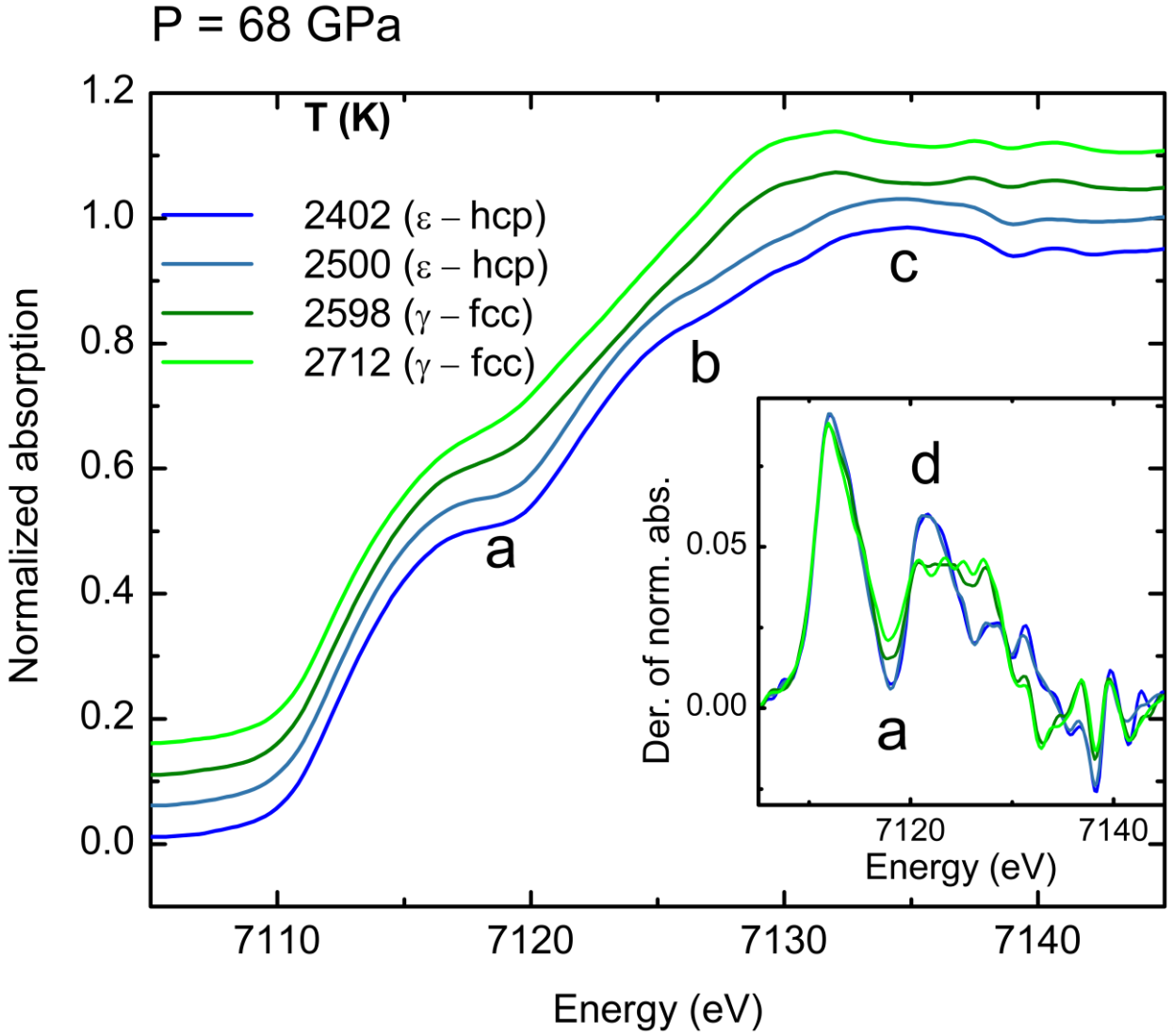

Aquilanti et al. (2015) *PNAS* **112**, 12042

giuliana.aquilanti@elettra.eu

Solid to liquid phase transition

- The modification of the onset of the absorption can be used a signature for the solid to liquid phase transition
- The onset of the absorption shows a discontinuous (although subtle) behavior
- The derivatives of the XANES highlight this change with the minimum ‘a’ flattening abruptly

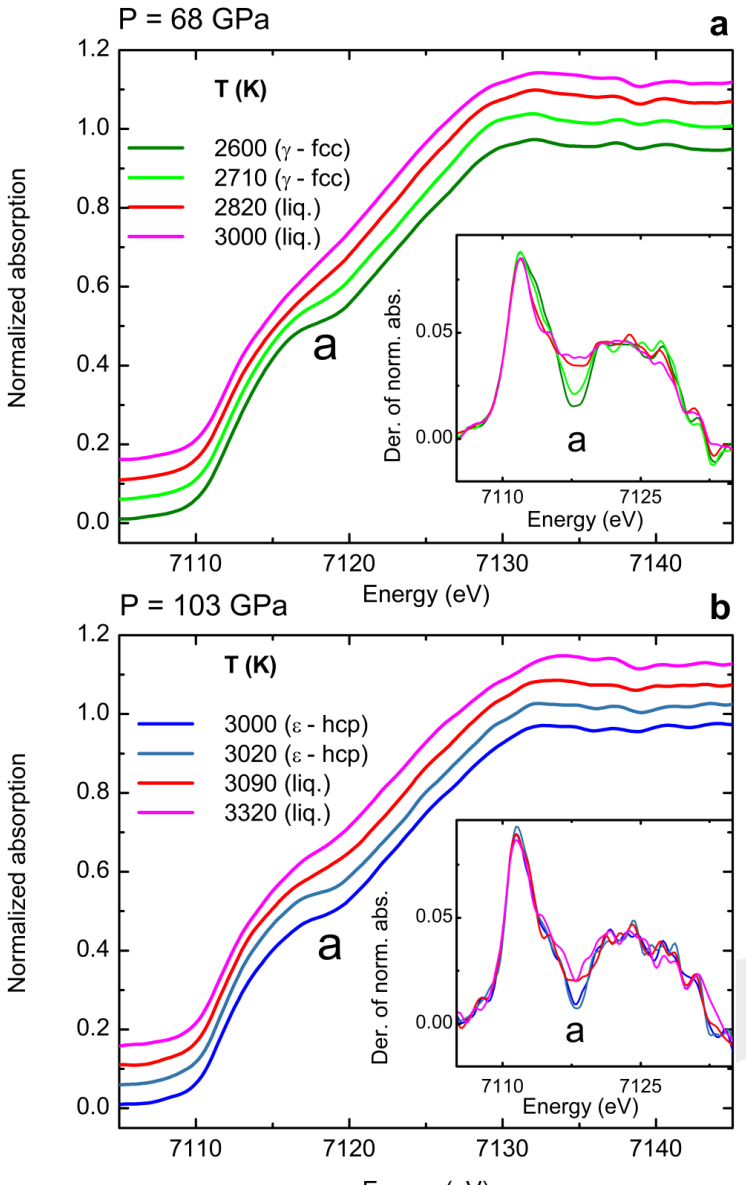

Aquilanti et al. (2015) *PNAS* **112**, 12042

giuliana.aquilanti@elettra.eu

Discussion

- The XAS experiment provides continuous monitoring of the changes of both the atomic and electronic structure as a function of temperature
- The melting criterion here adopted is based on changes occurring in the XANES that is known to be less affected by thermal damping and by the noise associated with extreme experimental conditions
- The detection of the new phase does not appear gradually as a weak background superimposed to a much larger signal as in XRD methods, but as a discontinuous change in the XANES signal which has similar amplitude with respect to that in the solid phase.

Aquilanti et al. (2015) *PNAS* **112**, 12042

Other transition metals

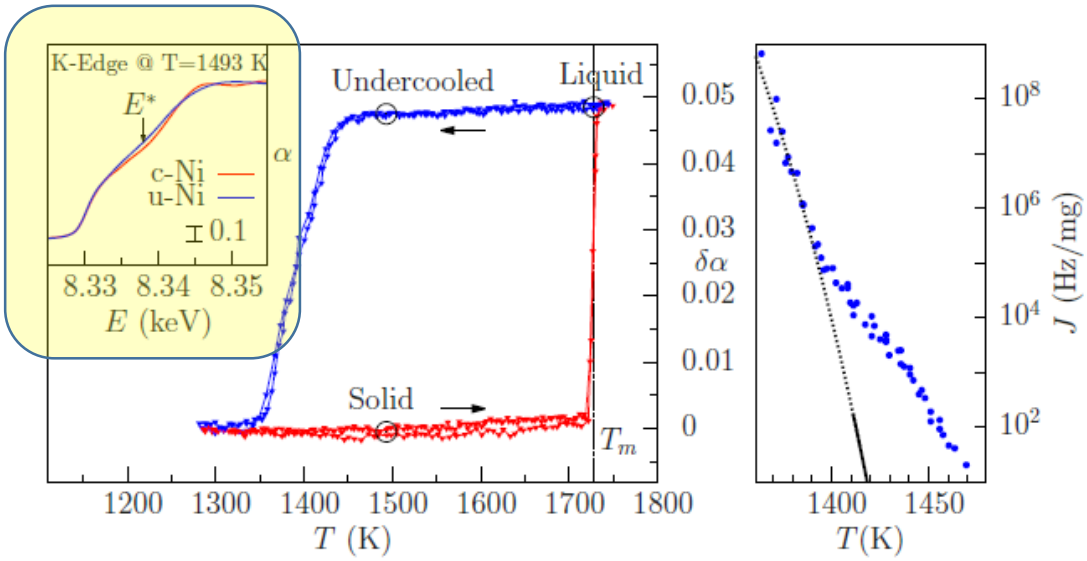

Nickel

Di Cicco et al. (2014)

PRB **89** 060102

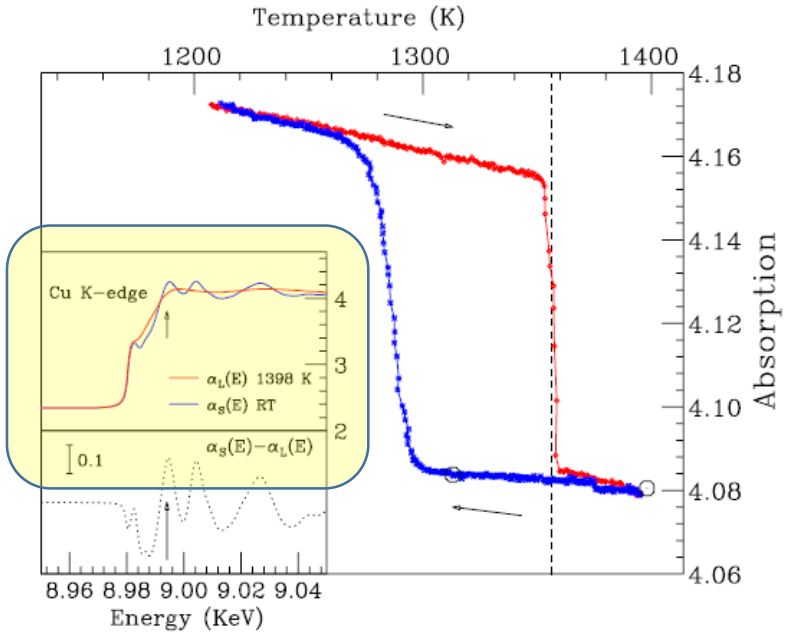

Copper

Di Cicco and Trapananti (2007)

J. Non Cryst. Sol. **353** 3671

Elettra Sincrotrone Trieste

XANES simulations

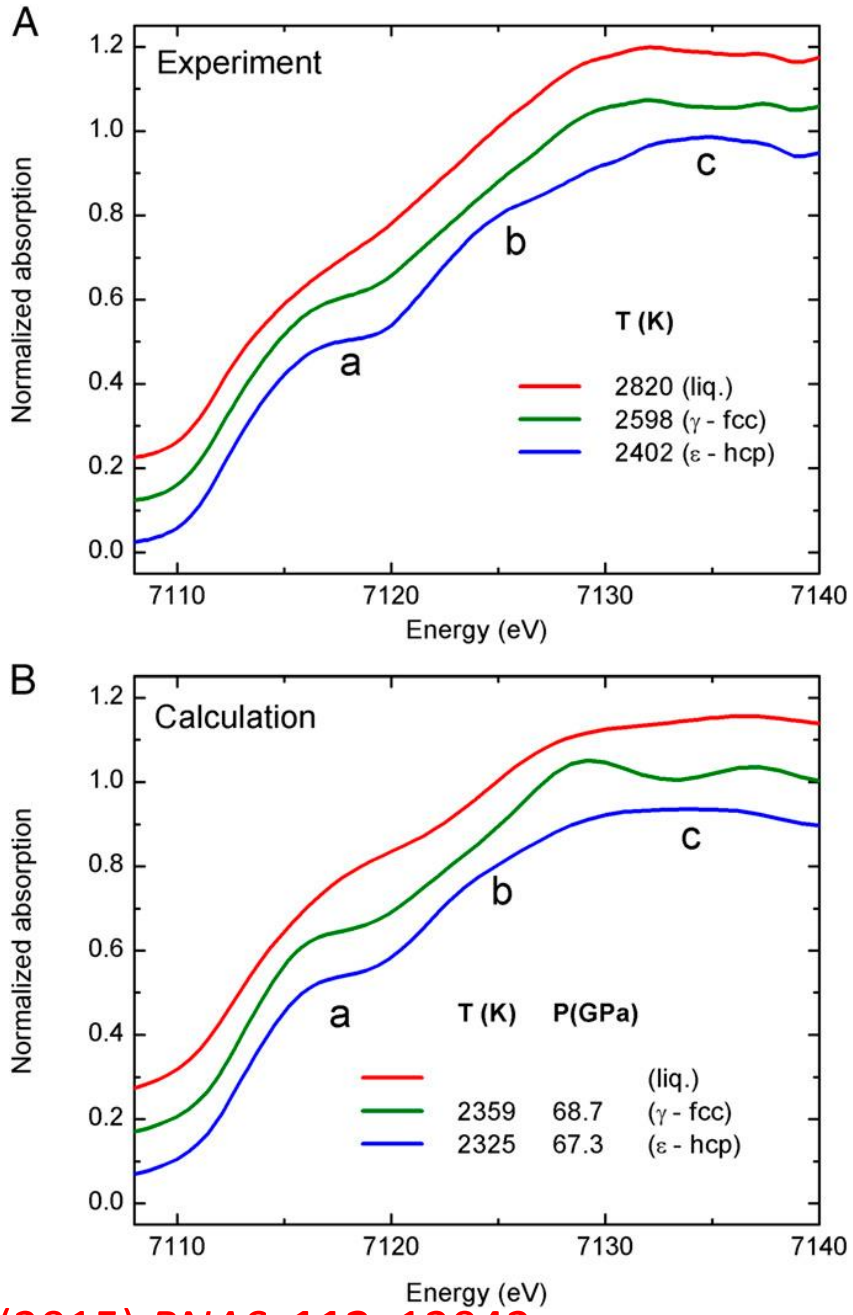

Aquilanti et al. (2015) *PNAS* **112**, 12042

Cu^{2+}-loaded Cu hexacyanoferrate

M. Giorgetti et al., PCCP **14**, 5527 (2012),
M. Giorgetti et al., J. Phys.: Conf. Series 430, 012049 (2013)

$A_xM_y[Fe(CN)_6]\cdot zH_2O$

"soluble"* structure (F-43m)

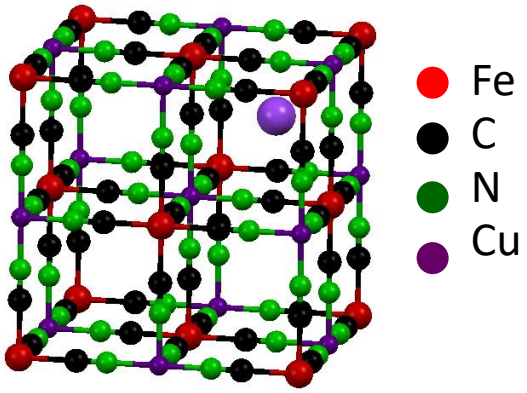

- a ~ 10.2 Å
- alkaly metals occupy intertitial 8c positions
- **-CN-Cu-NC-Fe-CN-** linear chains
- Fe and Cu in octahedral sites
  6 x Fe-CN-Cu
  6 x Cu-NC-Fe

"insoluble" * structure (Pm-3m)

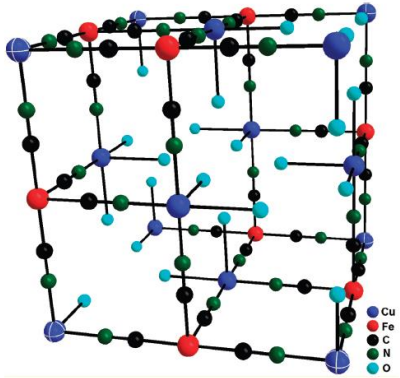

- Model with $[Fe(CN)_6]^{3-}$ ion vacancies

6 x Fe-CN-Cu
4.5 x Cu-NC-Fe
1.5 x Cu-O

Cu^{2+}-loaded Cu hexacyanoferrate: interest

Applications

- Electrochromism
- Electrocatalysis
- Ionic and electronic conductivity
- Charge storage
- Photo-induced magnetisation
- Electro-catalytic oxidation of alcohols in alkaline medium

Aim of the study

- Relationship between structure and properties
- **Amount of vacancies linked to the ability of H storage**

Data analysis strategy

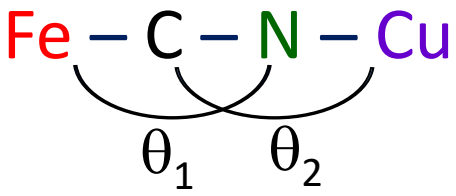

Linear chains between Cu and Fe gives rise to a *superfocusing effect* and therefore to a *large EXAFS signal*

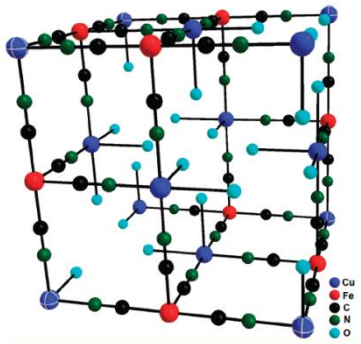

➡ Information on the amount of the vacancies

Signals for the Cu K-edge (CN)	
Two body	$\gamma_1^{(2)}$ Cu-N; (4.5)
	$\gamma_2^{(2)}$ Cu-O; (1.5)
	$\gamma_3^{(2)}$ Cu-K; (*)
Three body	$\eta_1^{(3)}$ Cu-N-C; (4.5)
Four body	$\eta_1^{(4)}$ Cu-N-C-Fe; (4.5)

Copper Hexacyanoferrate: Fe – C – N – Cu

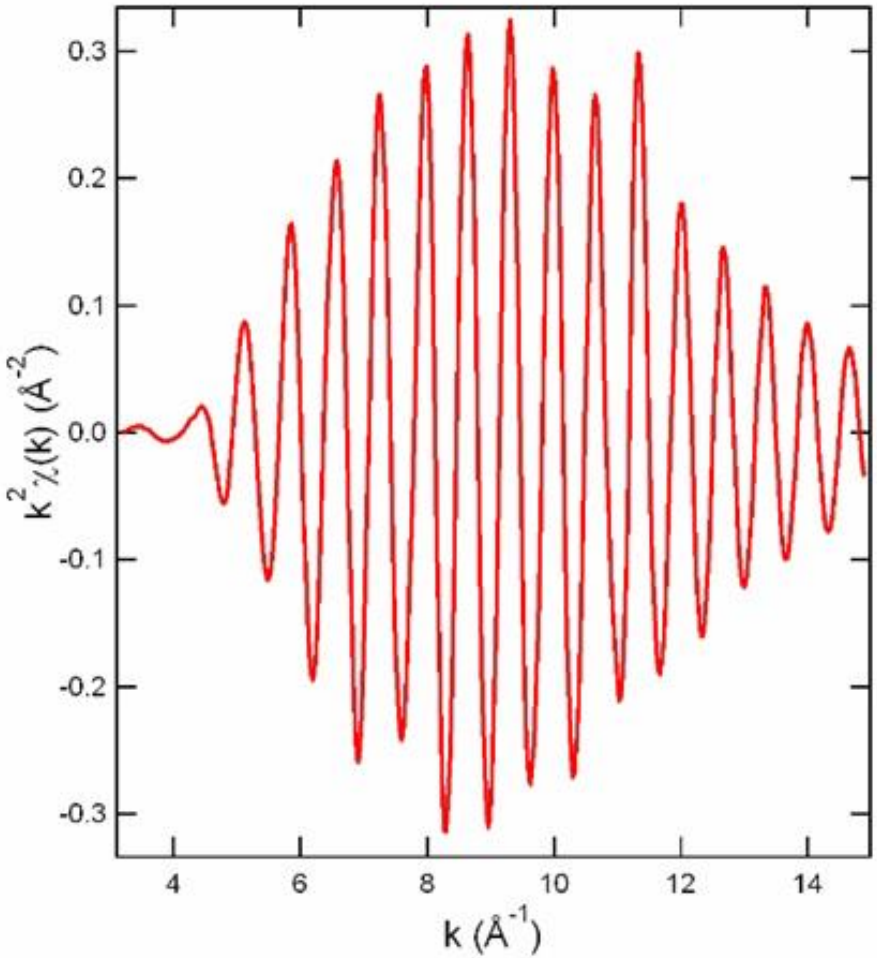

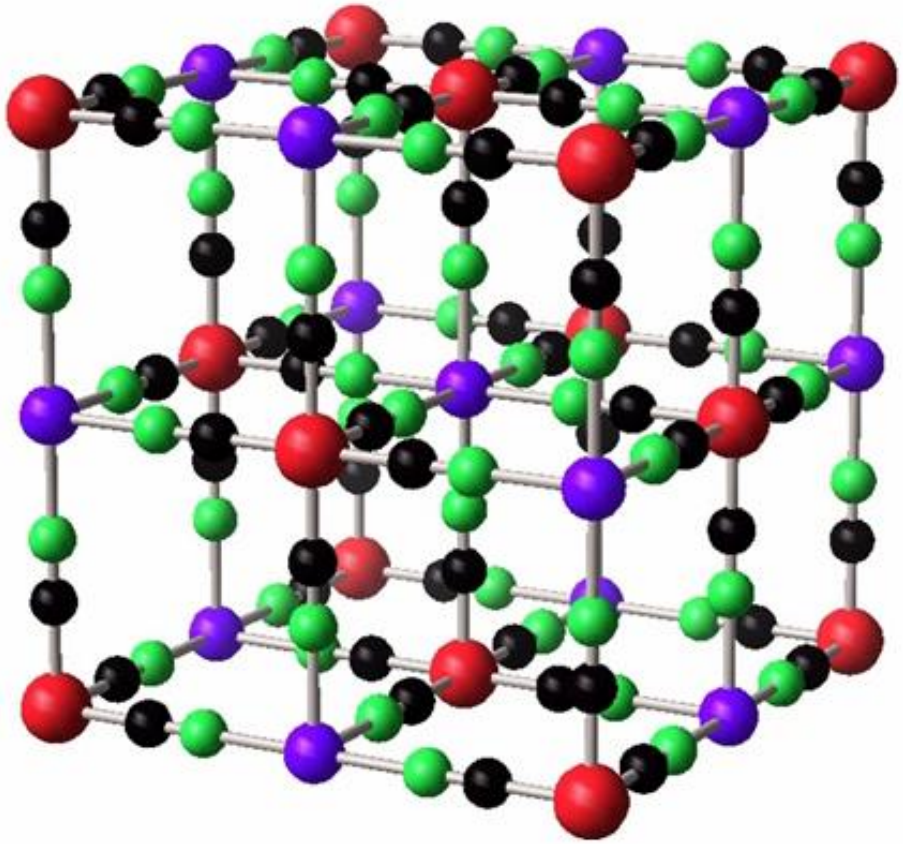

Copper Hexacyanoferrate: Fe – C – N – Cu

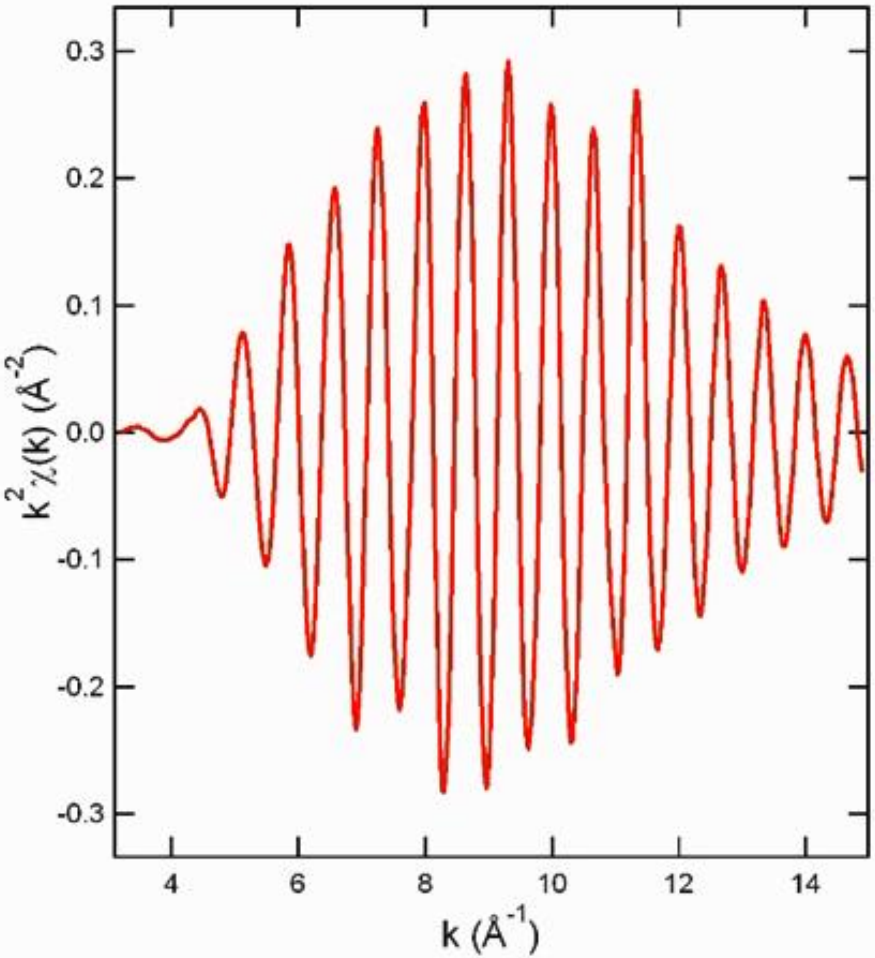

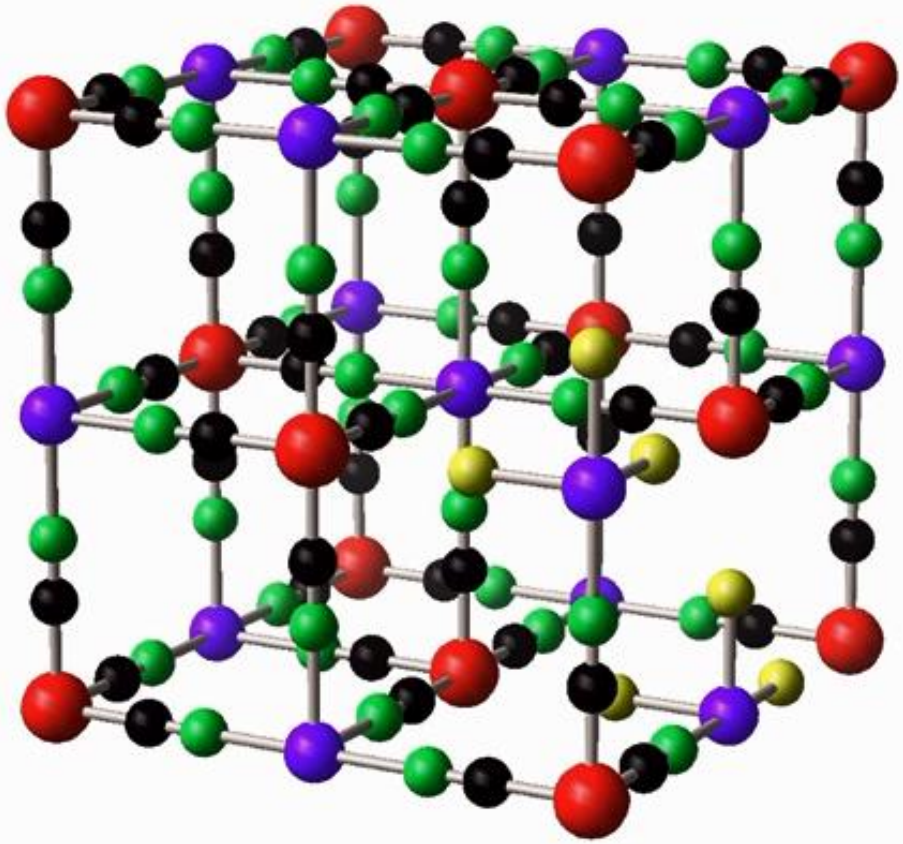

Copper Hexacyanoferrate: Fe – C – N – Cu

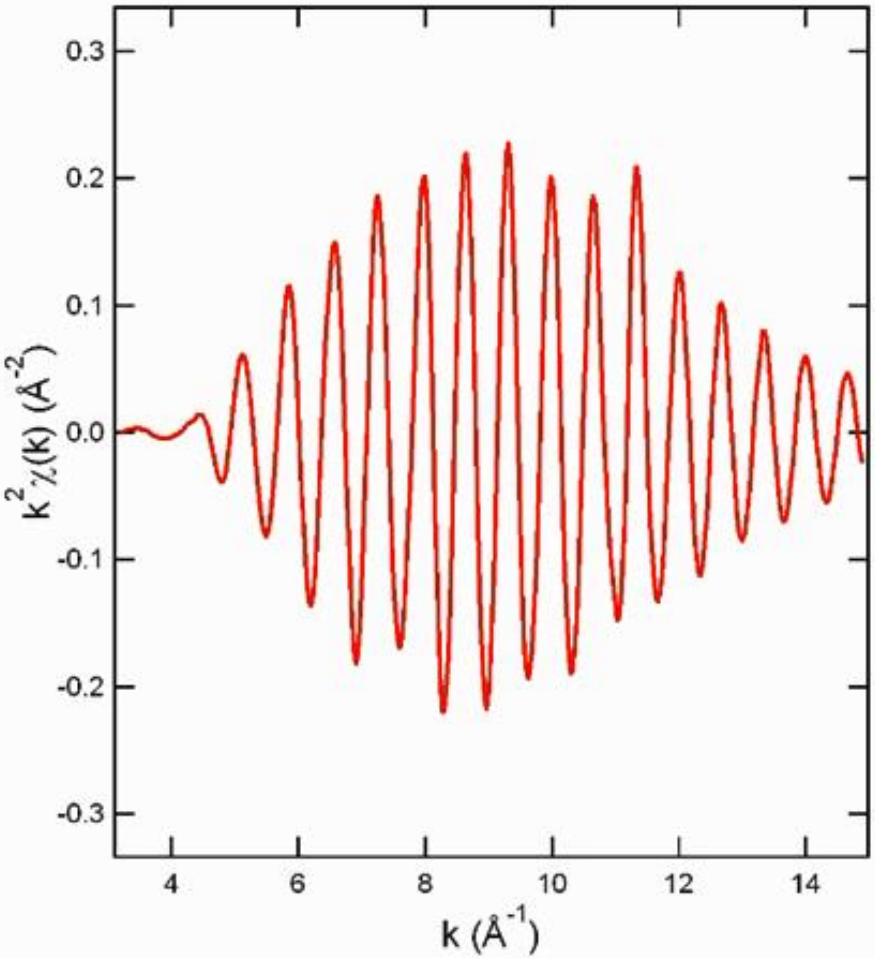

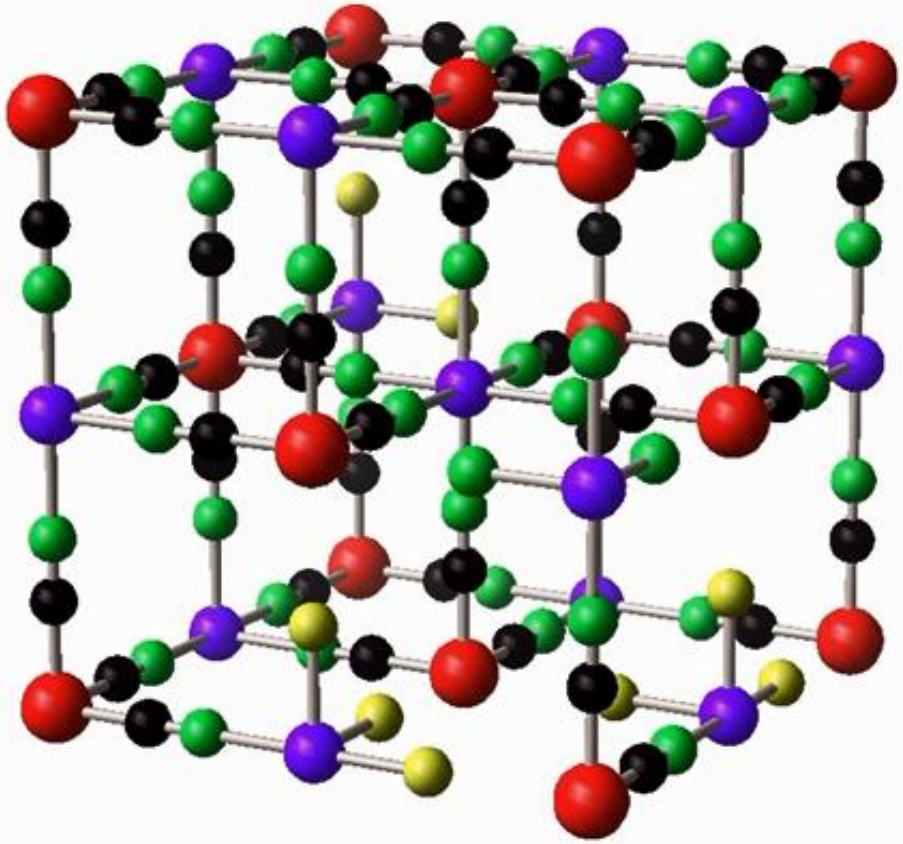

Copper Hexacyanoferrate: Fe – C – N – Cu

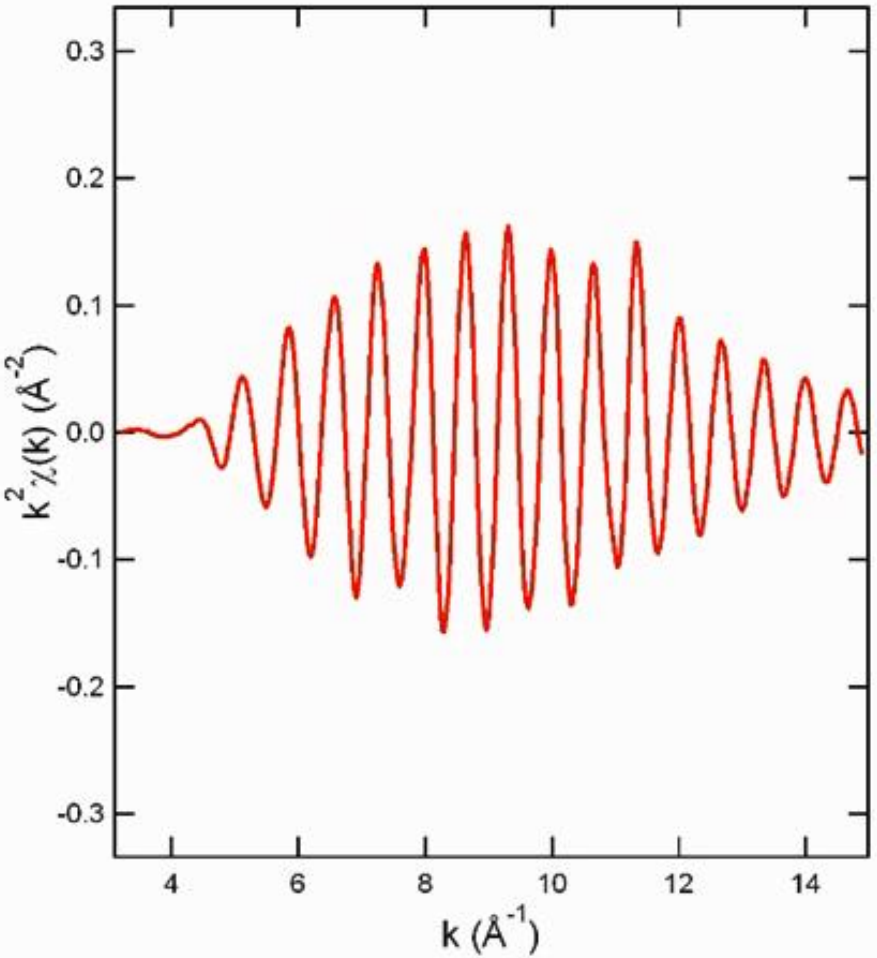

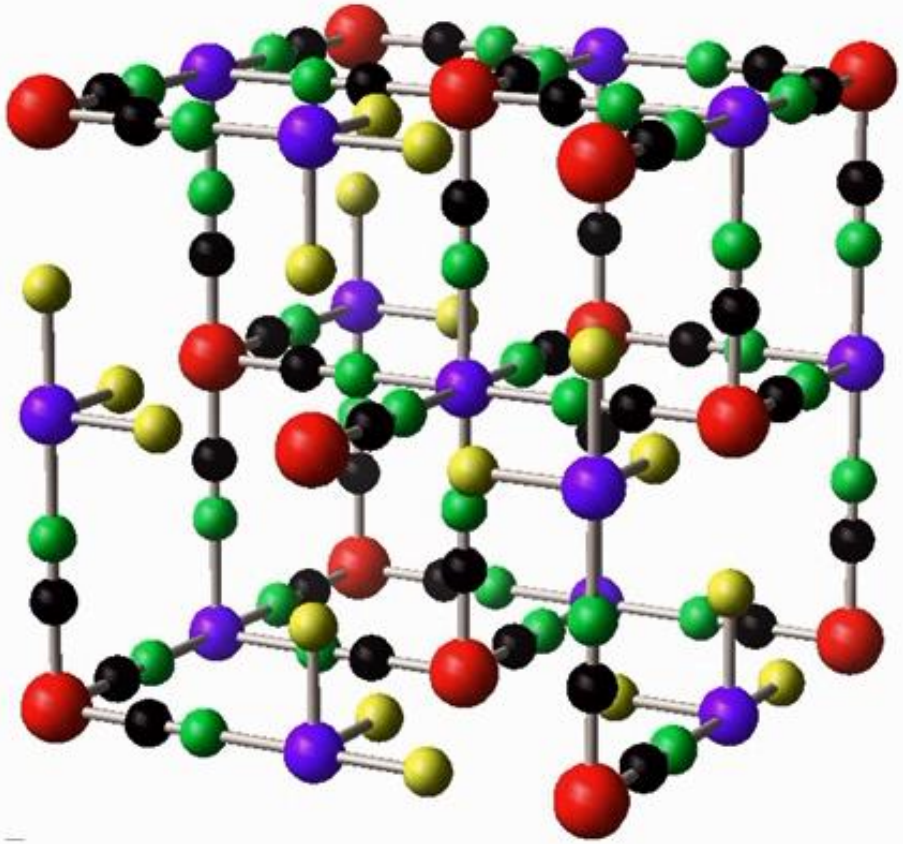

Copper Hexacyanoferrate: Fe – C – N – Cu

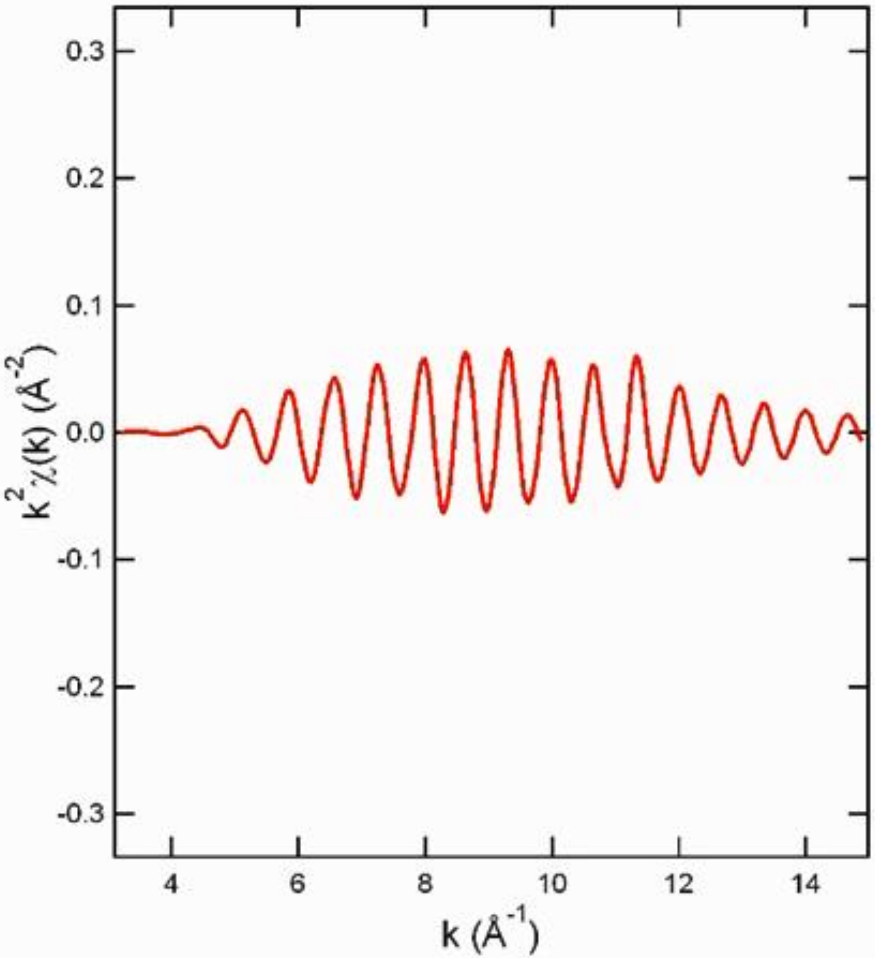

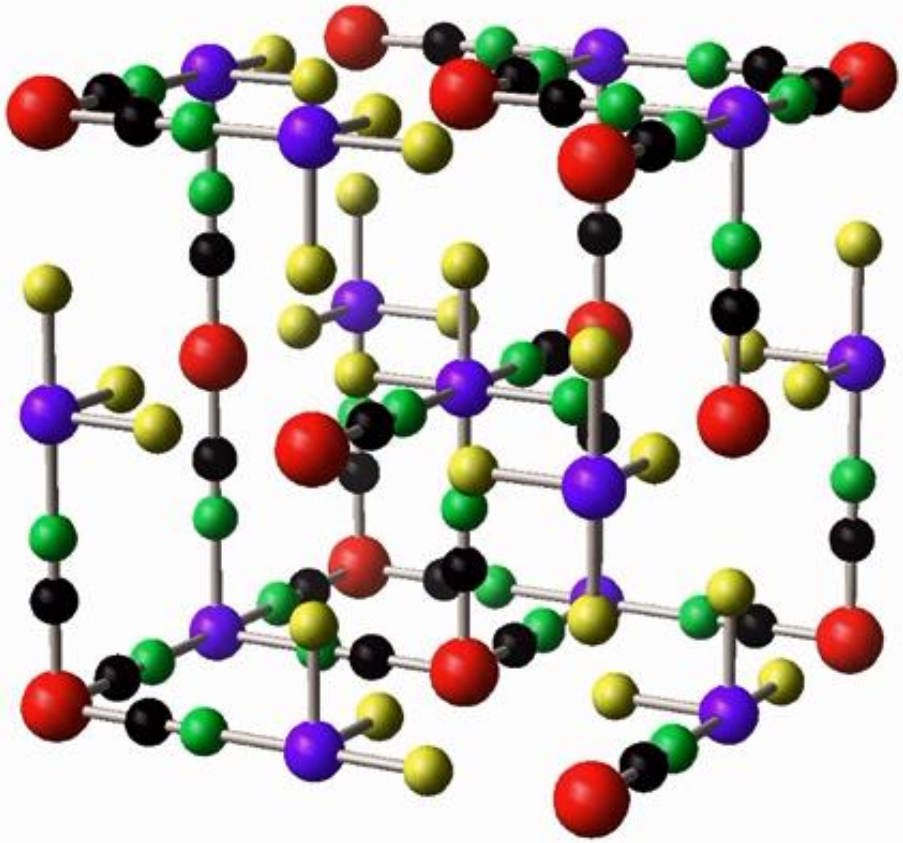

Fitting results

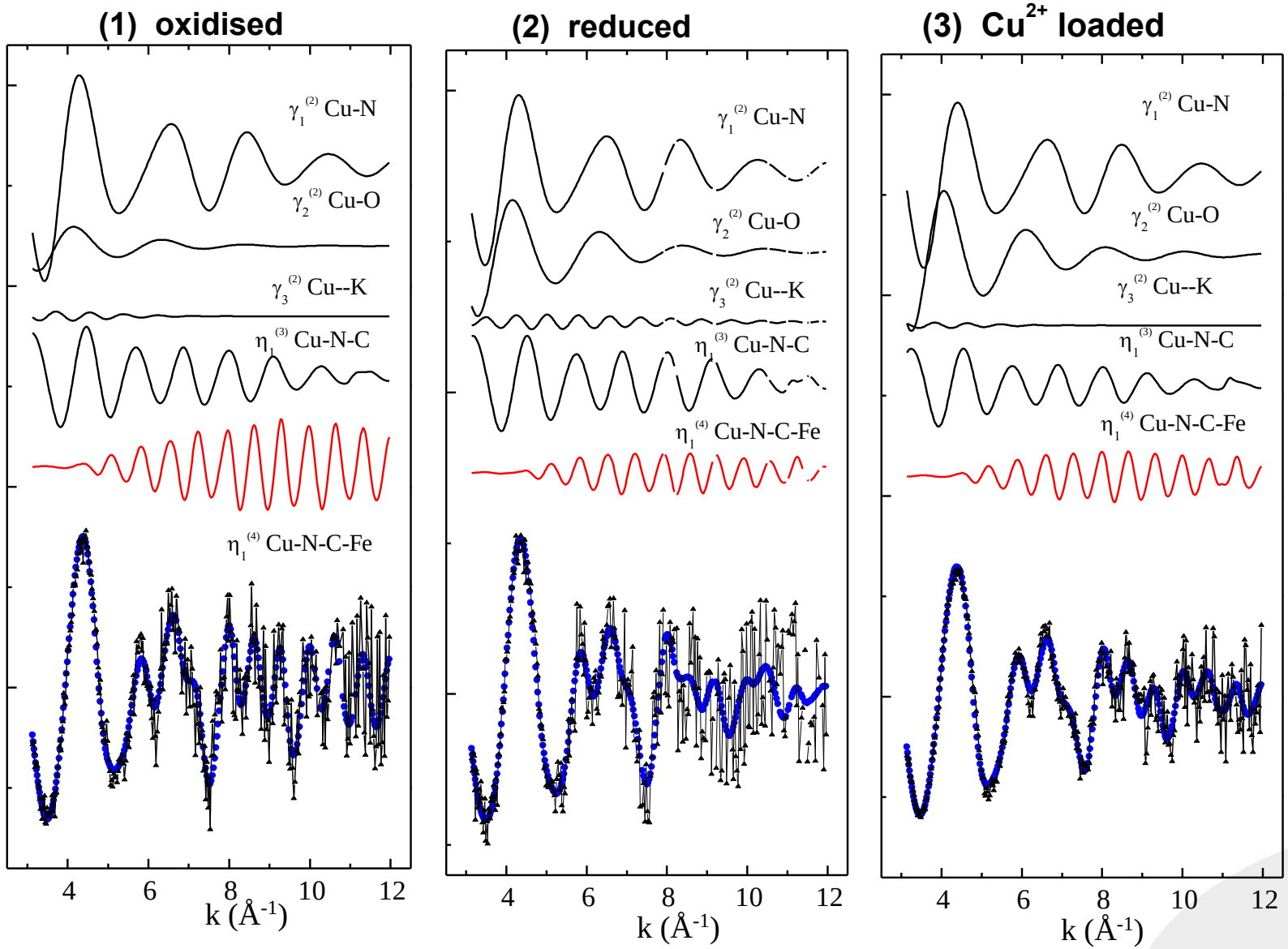

giuliana.aquilanti@elettra.eu

XAS applied to historical glasses

- Historical vitreous materials were highly appreciated because of their optical properties.
- Interplay between transparency, opacity, color, metallic shine, colored iridescence.
- Such effects can be induced by the presence of opacifying crystals, ionic chromophores, metallic nanoparticles
- The oxidation state of elements and more generally their chemical environment within the vitreous matrix is directly correlated to these optical effects.
- The historical production method therefore required adequate control of firing conditions (temperature, atmosphere, and time), as well as the introduction of oxidizing or reducing ingredients

Coloring variations are usually obtained in glass by modulating the oxidation states of transition elements such as Mn, Fe, Co, and Cu; these elements have characteristic absorption frequencies in the visible region as a result of d-d electronic transitions

Fe and Mn K-edge XANES study of ancient Roman glasses

- Study of ancient glasses from Patti Roman Villa (Messina, Sicily)
- From the chemical point of view, the samples are 'low-magnesia' glasses, with a composition typical of the Roman period
- Glasses of different colors from light green to pale brown
- Fe and Mn K-edge XANES

Aim of the work

- To test the influence of iron oxidation state on the color of the studied samples
- To identify the possible decolorant role of manganese oxide in the almost uncolored samples

S. Quartieri et al., Eur. J. Min. (2002) 14(4),749-756

Fe and Mn K-edge XANES study of ancient Roman glasses

Fragments of perfume bottles (2nd century AD)

S. Quartieri et al., Eur. J. Min. (2002) 14(4),749-756

Fe and Mn K-edge XANES study of ancient Roman glasses

Glass A: pale green

Glass B: uncolored

Glass C: pale brown

- B and C similar to each other: both in the general Shape and in the energy position of the different features
- Features (b) and (d) fall at high energy characteristic of Fe^{3+}

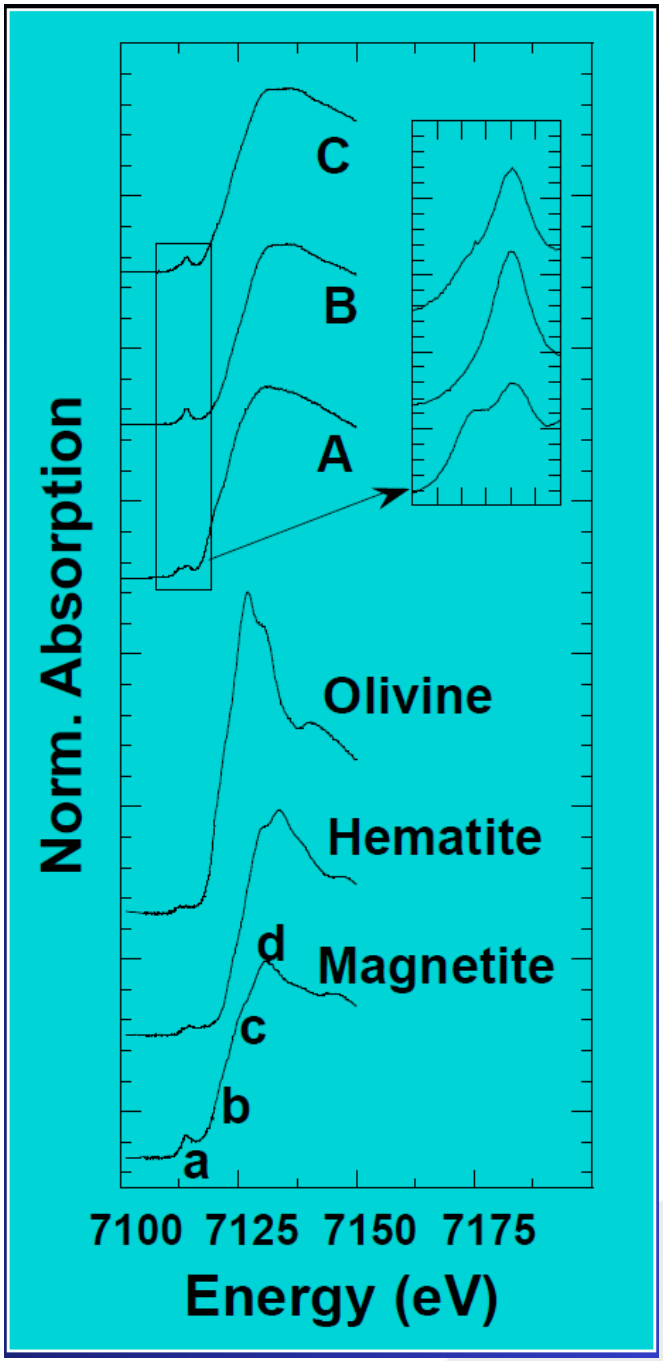

S. Quartieri et al., Eur. J. Min. (2002) 14(4),749-756

Fe and Mn K-edge XANES study of ancient Roman glasses

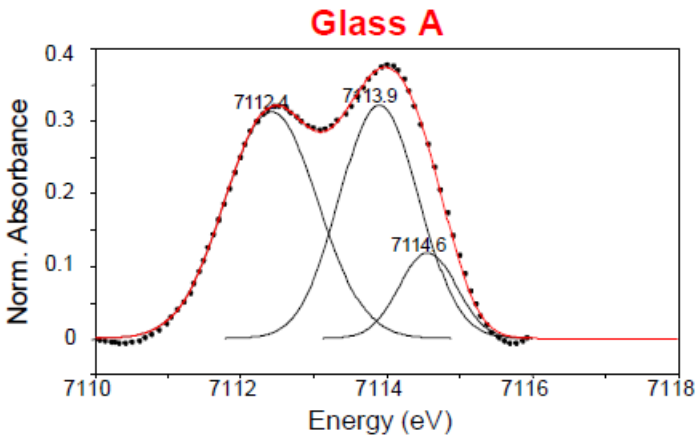

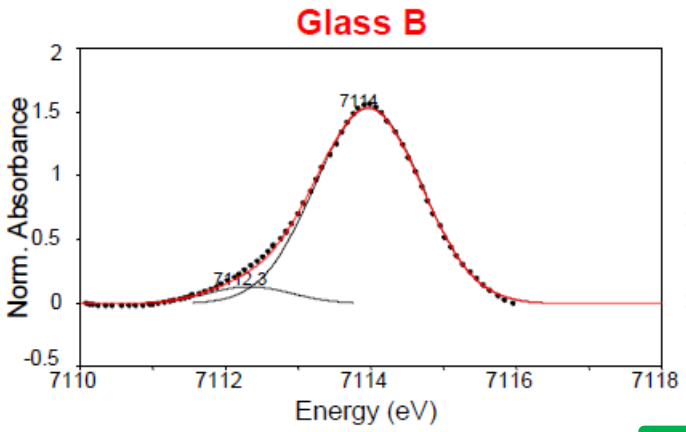

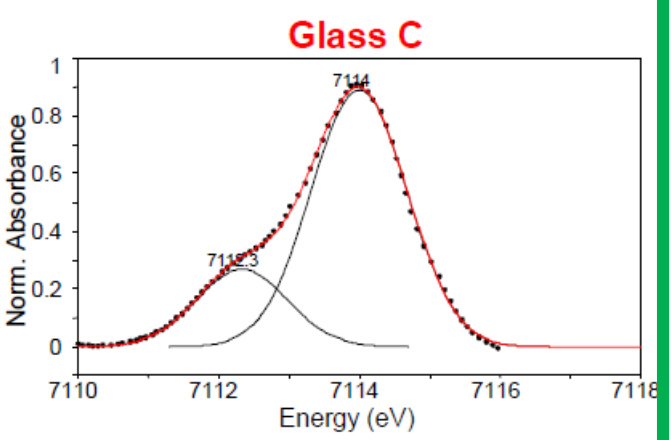

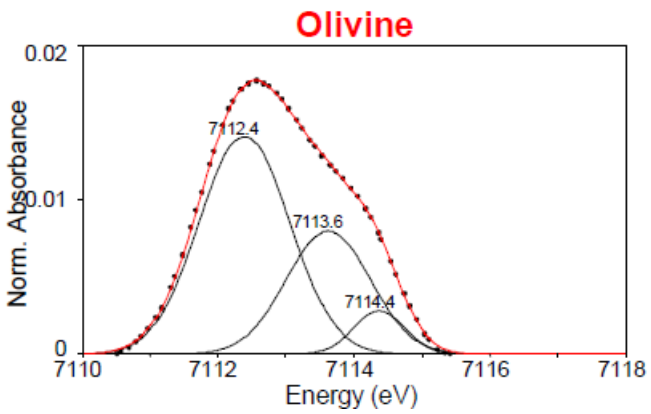

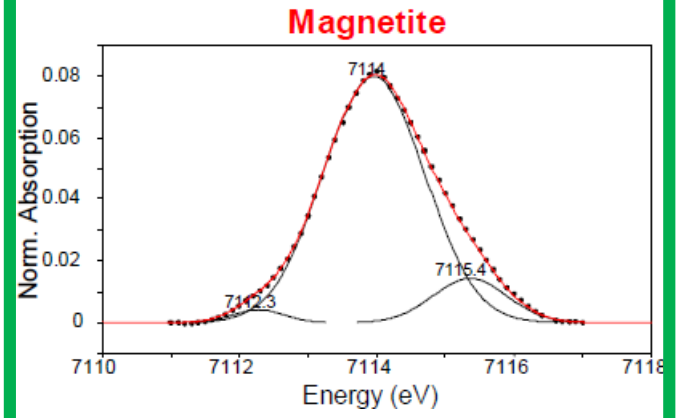

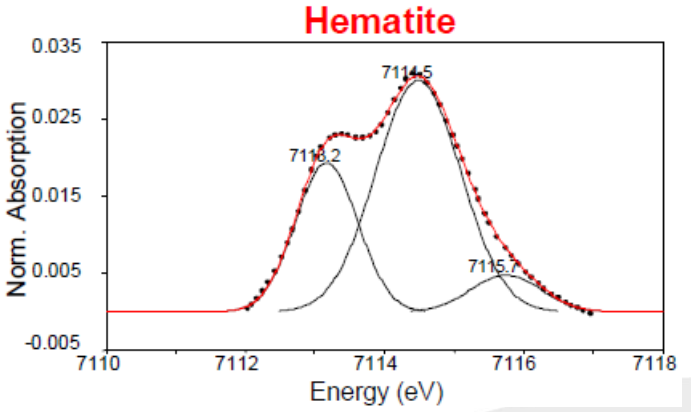

S. Quartieri et al., Eur. J. Min. (2002) 14(4),749-756

Fe and Mn K-edge XANES study of ancient Roman glasses

Glass A: pale green

Glass B: uncolored

Glass C: pale brown

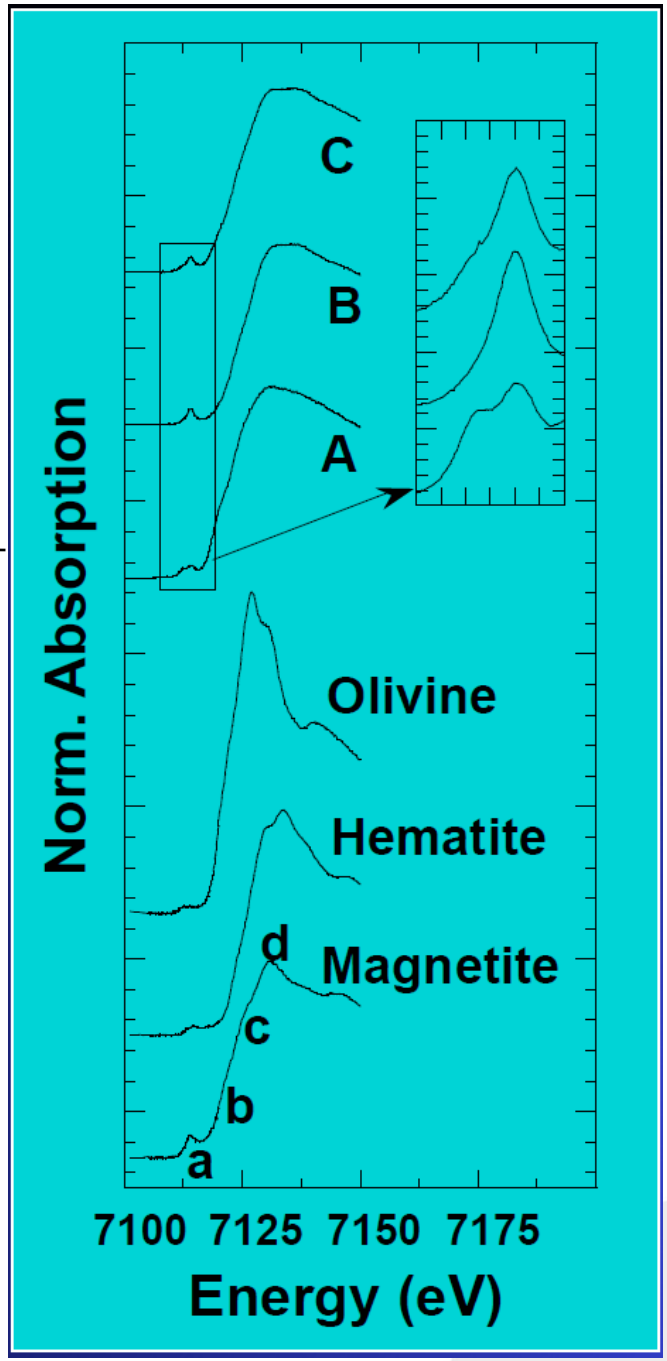

- In sample A the features (b) and (d) are at much lower energy, nearer to those present in the olivine spectrum characteristic of Fe^{+2}

S. Quartieri et al., Eur. J. Min. (2002) 14(4),749-756

Fe and Mn K-edge XANES study of ancient Roman glasses

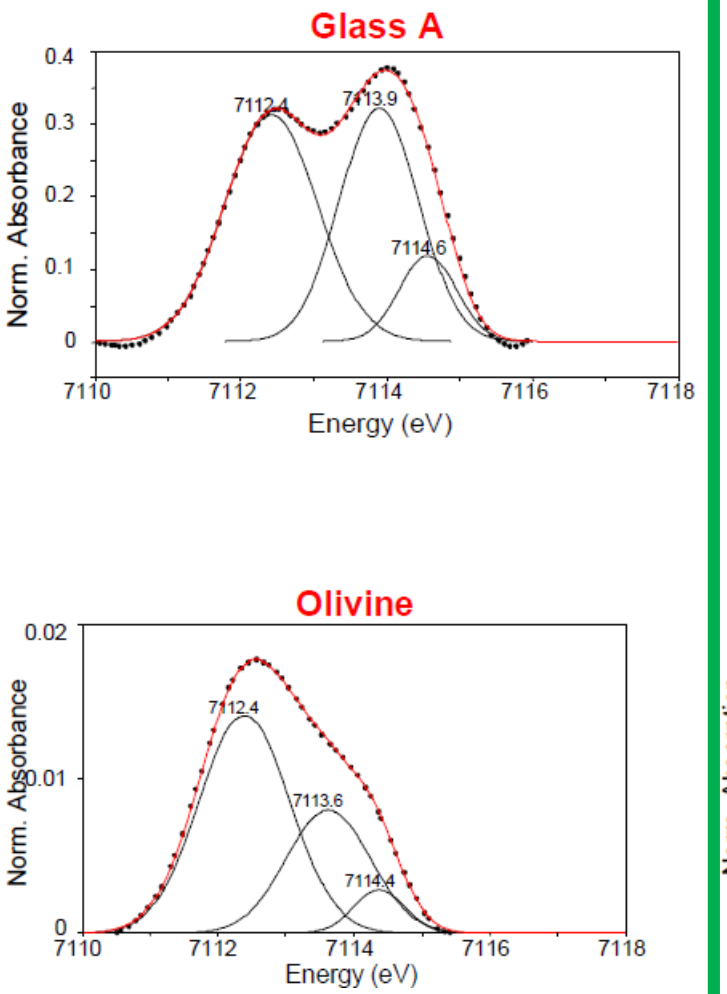

S. Quartieri et al., Eur. J. Min. (2002) 14(4),749-756

Fe and Mn K-edge XANES study of ancient Roman glasses

Glass A: pale green
Glass B: uncolored
Glass C: pale brown

- In glass C and in glass B, Fe is predominantly in 3+ oxidation state
- In glass A there is a high percentage of Fe^{2+}

S. Quartieri et al., Eur. J. Min. (2002) 14(4),749-756

Fe and Mn K-edge XANES study of ancient Roman glasses

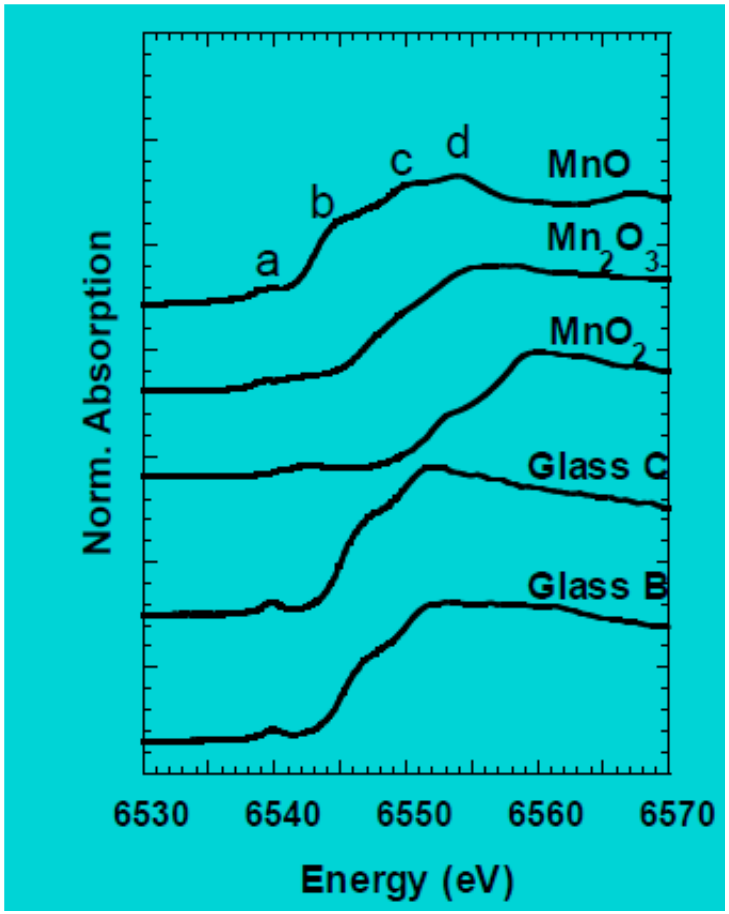

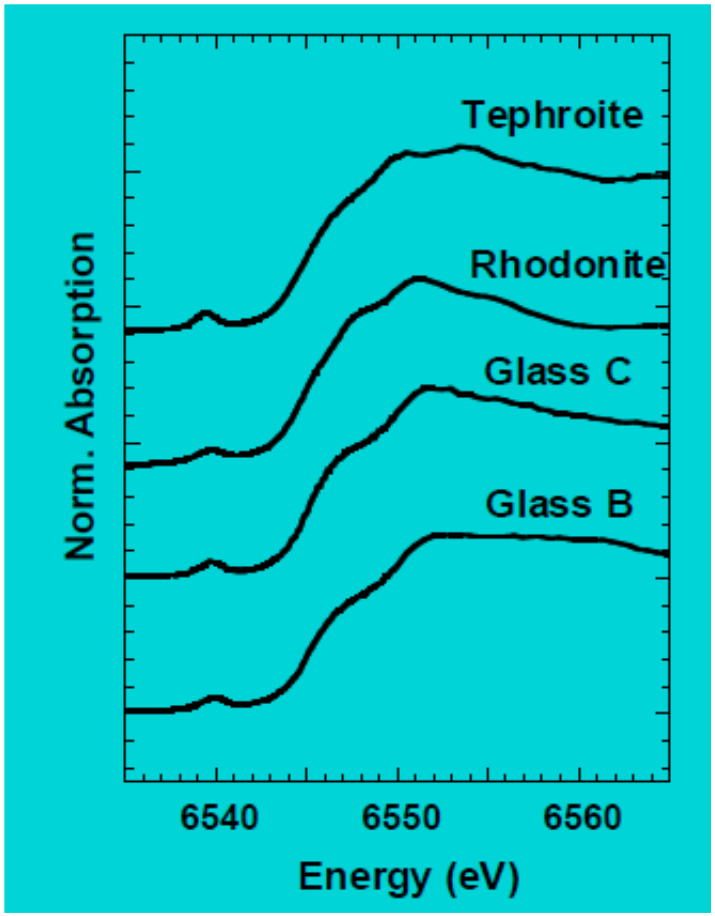

- Mn is in reduced form
- Strong similarity between the two Mn^{2+}-silicatic reference compounds

Fe and Mn K-edge XANES study of ancient Roman glasses

Glass A: pale green
Glass B: uncolored
Glass C: pale brown

Conclusion

- In sample B and C, Mn^{4+} has oxidised Fe^{2+} to Fe^{3+} and therefore is present in the reduced form
- It is confirmed the hypothesis of a redox interaction between manganese and iron as a results of a deliberate addition of pyrolusite (mineral containing MnO_2) – reported in literature as the main decolorant in the Roman period – during the melting procedure of the uncolored glass

S. Quartieri et al., Eur. J. Min. (2002) 14(4),749-756